



A fractional analysis of Noyes–Field model for the nonlinear Belousov–Zhabotinsky reaction

Lanre Akinyemi¹

Received: 25 December 2019 / Revised: 3 May 2020 / Accepted: 26 May 2020 / Published online: 9 June 2020
© SBMAC - Sociedade Brasileira de Matemática Aplicada e Computacional 2020

Abstract

Nonlinear phenomena play an essential role in various field of natural sciences and engineering. In particular, the nonlinear chemical reactions are observed in various domains, as, for instance, in biological and chemical physics. For this reason, it is important to investigate the solution to this nonlinear phenomenon. This article investigates numerical solutions to a nonlinear oscillatory system called the Belousov–Zhabotinsky with Caputo fractional-time derivative. The simplified Noyes–Field fractional model reads

$$\begin{aligned}\mathcal{D}_t^\mu p &= \xi_1 p_{xx} + \beta \delta w + p - p^2 - \delta pw, \quad 0 < \mu \leq 1, \\ \mathcal{D}_t^\mu w &= \xi_2 w_{xx} + \gamma w - \lambda pw,\end{aligned}$$

where ξ_1 and ξ_2 are the diffusing constants for the concentration p and w respectively, γ and β are given constants, $\lambda \neq 1$ and δ are positive parameters. The two iterative techniques used in this work are the fractional reduced differential transform method and q-homotopy analysis transform method. The outcomes using these two methods reveal an efficient numerical solution with high accuracy and minimal computations. Furthermore, to better understand the effect of the fractional order, we present the solution profiles which demonstrate the behavior of the obtained results.

Keywords Belousov–Zhabotinsky system · q-Homotopy analysis transform method · Laplace transform · Fractional reduced differential transform method · Fractional Fisher's equation

Mathematics Subject Classification 26A33 · 35Q92 · 35R11

1 Introduction

The applications of fractional calculus have been established in various connected bifurcation of science and engineering such as found in quantum mechanics Joseph (2012), random

Communicated by Agnieszka Malinowska.

✉ Lanre Akinyemi
la740411@ohio.edu

¹ Department of Mathematics, Ohio University, Athens, USA

walk Hilfer and Anton (1995), astrophysics Tarasov (2006), chaos theory Baleanu et al. (2017), electrodynamics Nasrolahpour (2013), viscoelasticity Mainardi (2010), nanotechnology Baleanu et al. (2010), financial models Sweilam et al. (2017) and other fields Ali et al. (2019), Sun et al. (2018), Baleanu et al. (2011), Kilbas et al. (2006), Kumar et al. (2018a), Jaradat et al. (2018b), Jaradat et al. (2018c), Laskin and Zaslavsky (2006), Pu (2007), Ullah et al. (2017) and Zhang et al. (2012). In the twentieth century, Caputo Caputo (1969), Liao Liao (1998), Podlubny Podlubny (1999) and Miller and Ross (1993) have described the essential properties of fractional calculus. Nonlinear problems with fractional order are often more difficult to solve because its operator is defined by integral. However, different computational schemes are developed and have been used to investigate both the exact and numerical solution of the fractional problems. Some of the used methods are the Adomian decomposition method, (ADM) Ray and Bera (2006), Adomian (1994) and Wazwaz and Gorguis (2004) variational iteration method, (VIM) Das (2009) and He (1998) homotopy perturbation method, (HPM) He (1999) and He (2003) residual power series method, (RPSM) Alquran et al. (2015), Kurt et al. (2019), Şenol et al. (2019a) and Şenol et al. (2019b) Sumudu decomposition method, (SDM), Eltayeb and Kilicman (2012), homotopy analysis method, (HAM) Liao (2004) and Liao (1995) Laplace decomposition method, (LDM) Khuri (2001) and q-homotopy analysis method, (q-HAM) Akinyemi (2019), Akinyemi et al. (2020), El-Tawil and Huseen (2012), El-Tawil and Huseen (2013), Iyiola (2015), Iyiola et al. (2013), Iyiola (2016) and Soh et al. (2014).

In this present work, we consider a nonlinear oscillatory system called the Belousov–Zhabotinsky, (B–Z) with Caputo fractional-time derivative. The B–Z is a family of oscillating chemical reactions and is interesting because this reaction is a chemical reaction which can demonstrate both temporal oscillations and spatial traveling concentration waves that are accompanied with dramatic color changes Gibbs (1980). This reaction can generate up to numerous thousand oscillatory cycles in a closed system that enables examining the chemical waves and patterns without constant replenishment of reactants Zhabotinsky Anatol (2007). The simplified Noyes–Field fractional model for this B–Z is given as

$$\begin{aligned}\mathcal{D}_t^\mu p &= \xi_1 p_{xx} + \beta \delta w + p - p^2 - \delta pw, \\ \mathcal{D}_t^\mu w &= \xi_2 w_{xx} + \gamma w - \lambda pw,\end{aligned}\tag{1}$$

where $0 < \mu \leq 1$ in Caputo sense and $0 < t < 1$. The motivation of this work is to study the numerical solutions of Eq. (1) with diffusing constants $\xi_1 = \xi_2 = 1$. Two distinct cases of Eq. (1) are considered.

- The first case is when $\gamma = \beta = 0$. This case has also been considered by Jaradat et al. (2018a) by means of generalized Taylor power series method with different initial conditions.
- The second case when $\gamma = \lambda$ and $\beta = 1$ is study for the first time.

In addition, to also examine graphically the effect of the fractional order μ on the obtained numerical solutions. The two methods proposed for this present investigation are the fractional reduced differential transform method, (FRDTM) and q-homotopy analysis transform method, (q-HATM). The FRDTM was proposed by Keskin and Oturanc (2010) while the q-HATM which is a combination of q-HAM and Laplace transform was proposed by Singh et al. (2018). These two methods overcome a very huge computations that may arise in other methods used to obtain approximate and exact solutions to strong nonlinear problems with high accuracy and minimal computations.

The rest of the paper is organized as follows: Sect. 2 presents some important definitions and notations of fractional calculus and Laplace transform used in the present framework. In Sect. 3, the general idea of the proposed methods are detailed. Section 4 is concerned with the application of the proposed methods on two cases of time-fractional Belousov–Zhabotinsky system of equations. The numerical experiments and discussion are presented in Sect. 5. Finally, Sect. 6 gives the conclusion.

2 Preliminaries

Here, we present key concept of fractional calculus and Laplace transform, which are vital in the present framework.

Definition 1 Let $\eta \in \mathbb{R}$ and $\varphi \in \mathbb{N}$. A function p is said to be in the space \mathbb{C}_η if there exists $\alpha \in \mathbb{R}$, $\alpha > \eta$ and $f \in C[0, \infty)$ such that $p(t) = t^\alpha f(t)$, $\forall t \in \mathbb{R}^+$. Furthermore, $p \in \mathbb{C}_\eta^\varphi$ if $p^{(\varphi)} \in \mathbb{C}_\eta$ Luchko and Srivastava (1995).

Definition 2 The Riemann–Liouville fractional integral of order μ ($\mu \geq 0$) of a function $p \in \mathbb{C}_\eta$, $\eta \geq -1$, is given as Podlubny (1999), Luchko and Srivastava (1995) and Kilbas et al. (2006)

$$J_t^\mu p(t) = \frac{1}{\Gamma(\mu)} \int_0^t (t-\xi)^{\mu-1} p(\xi) d\xi, \quad \mu, t > 0, \quad (2)$$

where Γ denoted the classical gamma function and $J_t^0 p(t) = p(t)$. For example,

$$J_t^\mu t^\nu = \frac{\Gamma(\mu+1)}{\Gamma(\mu+1+\nu)} t^{\mu+\nu}. \quad (3)$$

Definition 3 In the Caputo's sense, for $p \in \mathbb{C}_\eta$, $\eta \geq -1$ and $\varphi - 1 < \mu \leq \varphi$, $\varphi \in \mathbb{N}$, the fractional derivative of $p(t)$ (denoted by $D_t^\mu p(t)$) is defined as Podlubny (1999); Kilbas et al. (2006)

$$D_t^\mu p(t) = \begin{cases} p^{(\varphi)}(t), & \mu = \varphi, \\ J_t^{\varphi-\mu} p^{(\varphi)}(t), & \varphi - 1 < \mu < \varphi, \end{cases} \quad (4)$$

where

$$J_t^{\varphi-\mu} p^{(\varphi)}(t) = \frac{1}{\Gamma(\varphi-\mu)} \int_0^t (t-\xi)^{\varphi-\mu-1} p^{(\varphi)}(\xi) d\xi, \quad \mu, t > 0. \quad (5)$$

Definition 4 The Laplace transform (denoted by \mathcal{L}) of a Riemann–Liouville fractional integral ($J_t^\mu p(t)$) and Caputo fractional derivative ($D_t^\mu p(t)$) of a function $p \in \mathbb{C}_\eta$ ($\eta \geq -1$) is given, respectively, as Caputo (1969) and Kilbas et al. (2006)

$$\begin{aligned} \mathcal{L}[J_t^\mu p(t)] &= s^{-\mu} \mathcal{L}[p(t)], \\ \mathcal{L}[D_t^\mu p(t)] &= s^\mu \mathcal{L}[p(t)] - \sum_{m=0}^{\varphi-1} s^{\mu-m-1} p^{(m)}(0^+), \quad \varphi - 1 < \mu \leq \varphi, \end{aligned} \quad (6)$$

where s is a parameter.

3 Analysis of the proposed methods

Consider the time-fractional Belousov–Zhabotinsky, (TFB-Z) Eq. (1) with the diffusing constants for the concentration, $\xi_1 = \xi_2 = 1$,

$$\begin{aligned}\mathcal{D}_t^\mu p &= \frac{\partial^2 p}{\partial x^2} + \beta \delta w + p - p^2 - \delta p w, \quad 0 < \mu \leq 1, \\ \mathcal{D}_t^\mu w &= \frac{\partial^2 w}{\partial x^2} + \gamma w - \lambda p w,\end{aligned}\tag{7}$$

subject to initial conditions

$$\begin{aligned}p(x, 0) &= g_1(x), \\ w(x, 0) &= g_2(x), \quad x \in \mathbb{R}.\end{aligned}\tag{8}$$

3.1 Analysis of FRDTM

Let the functions $p(x, t)$ and $w(x, t)$ in Eq. (7) be analytic and continuously differentiable in the domain of investigation. In regard to the properties of differential transform, functions $p(x, t)$ and $w(x, t)$ can be express as

$$\begin{aligned}p(x, t) &= \sum_{m=0}^{\infty} P_m(x) t^{m\mu}, \\ w(x, t) &= \sum_{m=0}^{\infty} W_m(x) t^{m\mu},\end{aligned}\tag{9}$$

where

$$\begin{aligned}P_m(x) &= \frac{1}{\Gamma(m\mu + 1)} \left[\frac{\partial^{m\mu} p(x, t)}{\partial t^{m\mu}} \right]_{t=0}, \\ W_m(x) &= \frac{1}{\Gamma(m\mu + 1)} \left[\frac{\partial^{m\mu} w(x, t)}{\partial t^{m\mu}} \right]_{t=0}.\end{aligned}\tag{10}$$

Here, μ is the fractional order and the t -dimensional spectrum functions $P_m(x)$ and $W_m(x)$ are, respectively, the transformed functions of $p(x, t)$ and $w(x, t)$. According to Table 1, the iteration formulas for Eq. (7) are

$$\begin{aligned}\frac{\Gamma(m\mu + \mu + 1)}{\Gamma(m\mu + 1)} P_{(m+1)}(x) &= \frac{\partial^2 P_m}{\partial x^2} + \beta \delta W_m + P_m - \sum_{r=0}^m P_r P_{m-r} - \delta \sum_{r=0}^m P_r W_{m-r}, \\ \frac{\Gamma(m\mu + \mu + 1)}{\Gamma(m\mu + 1)} W_{(m+1)}(x) &= \frac{\partial^2 W_m}{\partial x^2} + \gamma W_m - \lambda \sum_{r=0}^m P_r W_{m-r}, \quad m = 0, 1, 2, 3, \dots.\end{aligned}\tag{11}$$

From initial condition Eq. (8), we write

$$\begin{aligned}P_0(x) &= p(x, 0), \\ W_0(x) &= w(x, 0).\end{aligned}\tag{12}$$

Table 1 The essential operations of FRDTM

| Functional form | Transformed function |
|---|--|
| p | $P_m = \frac{1}{\Gamma(m\mu+1)} \left[\frac{\partial^{m\mu} p}{\partial t^{m\mu}} \right]_{t=0}$ |
| $v = \beta_1 p + \beta_2 w$ | $V_m = \beta_1 P_m + \beta_2 W_m, \beta_1$ and β_2 are constants |
| $v = pq$ | $V_m = \sum_{i=0}^m P_i W_{(m-i)} = \sum_{i=0}^m W_i P_{(m-i)}$ |
| $v = D_t^{r\mu} p$ | $V_m = \frac{\Gamma(m\mu+r\mu+1)}{\Gamma(m\mu+1)} P_{(m+r)}$ |
| $v = \frac{\partial^v p}{\partial x^v}$ | $V_m = \frac{\partial^v P_m}{\partial x^v}$ |
| $v = x^r t^s$ | $V_m = x^r \hat{\delta}(m-s), \hat{\delta}(m-s) = \begin{cases} 1, & m=s \\ 0, & m \neq s \end{cases}$ |
| $v = e^{\beta t}$ | $V_m = \frac{\beta^m}{m!}$ |

Substituting Eqs. (12) into (11), we obtain the $P_m(x)$ and $W_m(x)$ values. The inverse transformation of the sets $\{P_m(x)\}_{m=0}^K$ and $\{W_m(x)\}_{m=0}^K$ are, respectively,

$$\begin{aligned} P^{[K]}(x, t) &= \sum_{m=0}^K P_m(x) t^{m\mu}, \\ W^{[K]}(x, t) &= \sum_{m=0}^K W_m(x) t^{m\mu} \end{aligned} \quad (13)$$

and

$$\begin{aligned} p(x, t) &= \lim_{k \rightarrow \infty} P^{[K]}(x, t) = \sum_{m=0}^{\infty} P_m(x) t^{m\mu}, \\ w(x, t) &= \lim_{k \rightarrow \infty} W^{[K]}(x, t) = \sum_{m=0}^{\infty} W_m(x) t^{m\mu}, \end{aligned} \quad (14)$$

which gives the exact solution of Eq. (7).

3.2 Fundamental idea of the q-HATM

Here, the central idea of q-HATM Kumara et al. 2017; Kumar et al. 2018b and Akinyemi (2020) to TFB-Z system of equations is presented. We first begin by applying Laplace transform to both sides of Eq. (7) and after simplifying, we obtain

$$\begin{aligned} \mathcal{L}[p(x, t)] - \frac{1}{s} \{p(x, 0)\} - \frac{1}{s^\mu} \mathcal{L} \left[\frac{\partial^2 p}{\partial x^2} + \beta \delta w + p - p^2 - \delta p w \right] &= 0, \\ \mathcal{L}[w(x, t)] - \frac{1}{s} \{w(x, 0)\} - \frac{1}{s^\mu} \mathcal{L} \left[\frac{\partial^2 w}{\partial x^2} + \gamma w - \lambda p w \right] &= 0. \end{aligned} \quad (15)$$

To epitomize the idea of homotopy method Liao (1998), we construct zeroth-order deformation equations for $0 \leq q \leq \frac{1}{n}$, $n \geq 1$, as

$$\begin{aligned}(1-nq)\mathcal{L}\left(\Phi_1(x, t; q) - p_0(x, t)\right) &= \hbar q \mathcal{H}(x, t) \mathcal{N}^p\left(\Phi_1(x, t; q), \Phi_2(x, t; q)\right), \\ (1-nq)\mathcal{L}\left(\Phi_2(x, t; q) - w_0(x, t)\right) &= \hbar q \mathcal{H}(x, t) \mathcal{N}^w\left(\Phi_1(x, t; q), \Phi_2(x, t; q)\right),\end{aligned}\quad (16)$$

and define $\mathcal{N}^p\left(\Phi_1(x, t; q), \Phi_2(x, t; q)\right)$ and $\mathcal{N}^w\left(\Phi_1(x, t; q), \Phi_2(x, t; q)\right)$, respectively, as

$$\begin{aligned}\mathcal{N}^p\left(\Phi_1(x, t; q), \Phi_2(x, t; q)\right) &= \mathcal{L}[\Phi_1(x, t; q)] - \frac{1}{s}\left\{g_1(x)\right\} - \frac{1}{s^\mu}\mathcal{L}\left[\frac{\partial^2\Phi_1(x, t; q)}{\partial x^2}\right. \\ &\quad \left.+\beta\delta\Phi_2(x, t; q) + \Phi_1(x, t; q) - \Phi_1^2(x, t; q) - \delta\Phi_1(x, t; q)\Phi_2(x, t; q)\right], \\ \mathcal{N}^w\left(\Phi_1(x, t; q), \Phi_2(x, t; q)\right) &= \mathcal{L}[\Phi_2(x, t; q)] - \frac{1}{s}\left\{g_2(x)\right\} - \frac{1}{s^\mu}\mathcal{L}\left[\frac{\partial^2\Phi_2(x, t; q)}{\partial x^2}\right. \\ &\quad \left.+\gamma\Phi_2(x, t; q) - \lambda\Phi_1(x, t; q)\Phi_2(x, t; q)\right],\end{aligned}\quad (17)$$

where q is the embedded parameter, the non-zero \hbar is the auxiliary parameter, \mathcal{L} is the Laplace transform and $\mathcal{H}(x, t) \neq 0$ represents the auxiliary function. Considering Eq. (16) with $q = 0, \frac{1}{n}$, we get

$$\begin{aligned}\Phi_1\left(x, t; 0\right) &= p_0(x, t), & \Phi_1\left(x, t; \frac{1}{n}\right) &= p(x, t), \\ \Phi_2\left(x, t; 0\right) &= w_0(x, t), & \Phi_2\left(x, t; \frac{1}{n}\right) &= w(x, t).\end{aligned}\quad (18)$$

When q rises from 0 to $\frac{1}{n}$, the solutions $\Phi_i(x, t; q)$, $i = 1, 2$, ranges from the initial guess p_0 and w_0 to the solution p and w . The Taylor series expansion of $\Phi_1(x, t; q)$ and $\Phi_2(x, t; q)$ are given as

$$\begin{aligned}\Phi_1(x, t; q) &= p_0(x, t) + \sum_{m=1}^{\infty} p_m(x, t) q^m, \\ \Phi_2(x, t; q) &= w_0(x, t) + \sum_{m=1}^{\infty} w_m(x, t) q^m,\end{aligned}\quad (19)$$

where

$$\begin{aligned}p_m(x, t) &= \frac{1}{m!} \left. \frac{\partial^m \Phi_1(x, t; q)}{\partial q^m} \right|_{q=0}, \\ w_m(x, t) &= \frac{1}{m!} \left. \frac{\partial^m \Phi_2(x, t; q)}{\partial q^m} \right|_{q=0}.\end{aligned}\quad (20)$$

If we choose p_0 , w_0 , \hbar , and \mathcal{H} adequately so that Eq. (19) converges at $q = \frac{1}{n}$, then we attain the following result for Eq. (7) as

$$\begin{aligned} p(x, t) &= p_0(x, t) + \sum_{m=1}^{\infty} p_m(x, t) \left(\frac{1}{n} \right)^m, \\ w(x, t) &= w_0(x, t) + \sum_{m=1}^{\infty} w_m(x, t) \left(\frac{1}{n} \right)^m. \end{aligned} \quad (21)$$

Differentiating Eq. (16) m -times w.r.t to “q”, setting $q = 0$ and lastly, multiply by $\frac{1}{m!}$ gives

$$\begin{aligned} \mathcal{L}[p_m(x, t) - \chi_m^* p_{m-1}(x, t)] &= \hbar \mathcal{H}(x, t) \mathcal{R}_{1,m}(\mathbf{p}_{m-1}(x, t), \mathbf{w}_{m-1}(x, t)), \\ \mathcal{L}[w_m(x, t) - \chi_m^* w_{m-1}(x, t)] &= \hbar \mathcal{H}(x, t) \mathcal{R}_{2,m}(\mathbf{p}_{m-1}(x, t), \mathbf{w}_{m-1}(x, t)). \end{aligned} \quad (22)$$

Here, the vectors \mathbf{p}_k and \mathbf{w}_k is define as

$$\begin{aligned} \mathbf{p}_k(x, t) &= \{p_0(x, t), p_1(x, t), \dots, p_k(x, t)\}, \\ \mathbf{w}_k(x, t) &= \{w_0(x, t), w_1(x, t), \dots, w_k(x, t)\}. \end{aligned} \quad (23)$$

Application of inverse Laplace transform on Eq. (22) with $\mathcal{H}(x, t) = 1$ gives

$$\begin{aligned} p_m(x, t) &= \chi_m^* p_{m-1}(x, t) + \hbar \mathcal{L}^{-1}[\mathcal{R}_{1,m}(\mathbf{p}_{m-1}(x, t), \mathbf{w}_{m-1}(x, t))], \\ w_m(x, t) &= \chi_m^* w_{m-1}(x, t) + \hbar \mathcal{L}^{-1}[\mathcal{R}_{2,m}(\mathbf{p}_{m-1}(x, t), \mathbf{w}_{m-1}(x, t))], \end{aligned} \quad (24)$$

where $\mathcal{R}_{1,m}(\mathbf{p}_{m-1}(x, t), \mathbf{w}_{m-1}(x, t))$ and $\mathcal{R}_{2,m}(\mathbf{p}_{m-1}(x, t), \mathbf{w}_{m-1}(x, t))$ are defined, respectively, as follows:

$$\begin{aligned} \mathcal{R}_{1,m}(\mathbf{p}_{m-1}, \mathbf{w}_{m-1}) &= \mathcal{L}[p_{m-1}] - \left(1 - \frac{\chi_m^*}{n}\right) \frac{1}{s} \{g_1(x)\} - \frac{1}{s^\mu} \mathcal{L}\left[\frac{\partial^2 p_{m-1}}{\partial x^2}\right. \\ &\quad \left. + \beta \delta w_{m-1} + p_{m-1} - \sum_{r=0}^{m-1} p_r p_{(m-1-r)} - \delta \sum_{r=0}^{m-1} p_r w_{(m-1-r)}\right], \\ \mathcal{R}_{2,m}(\mathbf{p}_{m-1}, \mathbf{w}_{m-1}) &= \mathcal{L}[w_{m-1}] - \left(1 - \frac{\chi_m^*}{n}\right) \frac{1}{s} \{g_2(x)\} \\ &\quad - \frac{1}{s^\mu} \mathcal{L}\left[\frac{\partial^2 w_{m-1}}{\partial x^2} + \gamma w_{m-1} - \lambda \sum_{r=0}^{m-1} p_r w_{(m-1-r)}\right], \end{aligned} \quad (25)$$

and

$$\chi_m^* = \begin{cases} 0 & m \leq 1, \\ n & otherwise. \end{cases} \quad (26)$$

Hence, Eqs. (24) and (25) reduces to

$$\begin{aligned} p_m(x, t) &= (\hbar + \chi_m^*) p_{m-1} - \hbar \left(1 - \frac{\chi_m^*}{n}\right) \mathcal{L}^{-1}\left[\frac{1}{s} \{g_1(x)\}\right] - \hbar \mathcal{L}^{-1}\left[\frac{1}{s^\mu} \mathcal{L}\left[\frac{\partial^2 p_{m-1}}{\partial x^2}\right.\right. \\ &\quad \left.\left. + \beta \delta w_{m-1} + p_{m-1} - \sum_{r=0}^{m-1} p_r p_{(m-1-r)} - \delta \sum_{r=0}^{m-1} p_r w_{(m-1-r)}\right]\right], \end{aligned}$$

$$\begin{aligned} w_m(x, t) = & (\hbar + \chi_m^*) w_{m-1} - \hbar \left(1 - \frac{\chi_m^*}{n} \right) \mathcal{L}^{-1} \left[\frac{1}{s} \left\{ g_2(x) \right\} \right] \\ & - \hbar \mathcal{L}^{-1} \left[\frac{1}{s^\mu} \mathcal{L} \left[\frac{\partial^2 w_{m-1}}{\partial x^2} + \gamma w_{m-1} - \lambda \sum_{r=0}^{m-1} p_r w_{(m-1-r)} \right] \right], \quad m = 1, 2, 3, \dots \end{aligned} \quad (27)$$

The iterative terms of $p(x, t)$ and $w(x, t)$ are generated from simplifying Eq. (27) and the q-HATM series solution is

$$\begin{aligned} P^{[K]}(x, t; n; \hbar) &= \sum_{m=0}^K p_m(x, t) \left(\frac{1}{n} \right)^m, \\ W^{[K]}(x, t; n; \hbar) &= \sum_{m=0}^K w_m(x, t) \left(\frac{1}{n} \right)^m. \end{aligned} \quad (28)$$

Then for a prescribed value of n and \hbar ,

$$\begin{aligned} p(x, t) &= \lim_{k \rightarrow \infty} P^{[K]}(x, t; n; \hbar) = \sum_{m=0}^{\infty} p_m(x, t) \left(\frac{1}{n} \right)^m, \\ w(x, t) &= \lim_{k \rightarrow \infty} W^{[K]}(x, t; n; \hbar) = \sum_{m=0}^{\infty} w_m(x, t) \left(\frac{1}{n} \right)^m. \end{aligned} \quad (29)$$

Theorem 3.1 (El-Tawil and Huseen (2012) and Kumar et al. (2018b)) Suppose we can obtain real numbers \mathcal{M}_1 and \mathcal{M}_2 such that $0 < \mathcal{M}_1 < 1$ and $0 < \mathcal{M}_2 < 1$ satisfying

$$\|p_{m+1}(x, t)\| \leq \mathcal{M}_1 \|p_m(x, t)\|, \quad \|w_{m+1}(x, t)\| \leq \mathcal{M}_2 \|w_m(x, t)\|, \quad \forall m \in \mathbb{N}.$$

Furthermore, if the truncated series $P^{[K]}(x, t; n; \hbar)$ and $W^{[K]}(x, t; n; \hbar)$ defined in Eq. (28) are, respectively, used as an approximation to the solutions $p(x, t)$ and $w(x, t)$, then the maximum absolute truncated errors are estimated, respectively, as

$$\|p(x, t) - P^{[K]}(x, t; n; \hbar)\| \leq \frac{\mathcal{M}_1^{K+1}}{n^K(n - \mathcal{M}_1)} \|p_0(x, t)\| \quad (30)$$

and

$$\|w(x, t) - W^{[K]}(x, t; n; \hbar)\| \leq \frac{\mathcal{M}_2^{K+1}}{n^K(n - \mathcal{M}_2)} \|w_0(x, t)\|. \quad (31)$$

Proof For a prescribed value of n ($n \geq 1$) and \hbar ($\hbar \neq 0$), we have

$$\begin{aligned} \|p(x, t) - P^{[K]}(x, t; n; \hbar)\| &= \left\| \sum_{m=0}^{\infty} p_m(x, t) \left(\frac{1}{n} \right)^m - \sum_{m=0}^K p_m(x, t) \left(\frac{1}{n} \right)^m \right\| \\ &= \left\| \sum_{m=K+1}^{\infty} p_m(x, t) \left(\frac{1}{n} \right)^m \right\| \\ &\leq \sum_{m=K+1}^{\infty} \|p_m(x, t)\| \left(\frac{1}{n} \right)^m \end{aligned}$$

$$\begin{aligned}
&\leq \sum_{m=K+1}^{\infty} \mathcal{M}_1^m \|p_0(x, t)\| \left(\frac{1}{n}\right)^m \\
&\leq \sum_{m=K+1}^{\infty} \left(\frac{\mathcal{M}_1}{n}\right)^m \|p_0(x, t)\| \\
&\leq \left(\frac{\mathcal{M}_1}{n}\right)^{K+1} \left\{1 + \left(\frac{\mathcal{M}_1}{n}\right) + \left(\frac{\mathcal{M}_1}{n}\right)^2 + \dots\right\} \|p_0(x, t)\| \\
&\leq \frac{\mathcal{M}_1^{K+1}}{n^K(n - \mathcal{M}_1)} \|p_0(x, t)\|.
\end{aligned}$$

By following the same approach, we also obtain

$$\|w(x, t) - \mathbf{W}^{[K]}(x, t; n; \hbar)\| \leq \frac{\mathcal{M}_2^{K+1}}{n^K(n - \mathcal{M}_2)} \|w_0(x, t)\|.$$

This completes the proof. \square

4 Solution for TFB-Z system of equations

Here, application of the two proposed methods is tested on two cases of time-fractional Belousov–Zhabotinsky (TFB-Z) Eq. (7).

Case 1 Consider the nonlinear TFB-Z system with $\gamma = \beta = 0$, then Eq. (7) reduces to

$$\begin{aligned}
\frac{\partial^\mu p}{\partial t^\mu} &= \frac{\partial^2 p}{\partial t^2} + p - p^2 - \delta p w, \quad 0 < \mu \leq 1, \\
\frac{\partial^\mu w}{\partial t^\mu} &= \frac{\partial^2 w}{\partial t^2} - \lambda p w,
\end{aligned} \tag{32}$$

with the initial conditions

$$\begin{aligned}
p(x, 0) &= \frac{1}{\left(e^{\sqrt{\frac{\lambda}{6}}x} + 1\right)^2}, \\
w(x, 0) &= \frac{(1 - \lambda)e^{\sqrt{\frac{\lambda}{6}}x} \left(e^{\sqrt{\frac{\lambda}{6}}x} + 2\right)}{\delta \left(e^{\sqrt{\frac{\lambda}{6}}x} + 1\right)^2}.
\end{aligned} \tag{33}$$

The exact solution of Eq. (32) when $\mu = 1$ is

$$\begin{aligned}
p(x, t) &= \frac{e^{\frac{5\lambda}{3}t}}{\left(e^{\sqrt{\frac{\lambda}{6}}x} + e^{\frac{5\lambda}{6}t}\right)^2}, \\
w(x, t) &= \frac{(1 - \lambda)e^{\sqrt{\frac{\lambda}{6}}x} \left(e^{\sqrt{\frac{\lambda}{6}}x} + 2e^{\frac{5\lambda}{6}t}\right)}{\delta \left(e^{\sqrt{\frac{\lambda}{6}}x} + e^{\frac{5\lambda}{6}t}\right)^2}.
\end{aligned} \tag{34}$$

Here δ and $\lambda \neq 1$ are positive parameters.

Remark 1 The exact solution can also have the following form:

$$\begin{aligned} \frac{e^{\frac{5\lambda}{3}t}}{\left(e^{\sqrt{\frac{\lambda}{6}}x} + e^{\frac{5\lambda}{6}t}\right)^2} &= \frac{1}{4} \left(\tanh^2 \left(\sqrt{\frac{\lambda}{24}}x - \frac{5\lambda}{12}t \right) - 1 \right)^2, \\ \frac{(1-\lambda)e^{\sqrt{\frac{\lambda}{6}}x} \left(e^{\sqrt{\frac{\lambda}{6}}x} + 2e^{\frac{5\lambda}{6}t}\right)}{\delta \left(e^{\sqrt{\frac{\lambda}{6}}x} + e^{\frac{5\lambda}{6}t}\right)^2} &= \frac{\lambda-1}{4\delta} \left(\tanh^2 \left(\sqrt{\frac{\lambda}{24}}x - \frac{5\lambda}{12}t \right) - 2 \tanh \left(\sqrt{\frac{\lambda}{24}}x - \frac{5\lambda}{12}t \right) - 3 \right). \end{aligned} \quad (35)$$

FRDTM solution

From Eq. (11) with $\gamma = \beta = 0$, we have

$$\begin{aligned} P_{(m+1)}(x) &= \frac{\Gamma(m\mu+1)}{\Gamma(m\mu+\mu+1)} \left\{ \frac{\partial^2 P_m}{\partial x^2} + P_m - \sum_{r=0}^m P_r P_{m-r} - \delta \sum_{r=0}^m P_r W_{m-r} \right\}, \\ W_{(m+1)}(x) &= \frac{\Gamma(m\mu+1)}{\Gamma(m\mu+\mu+1)} \left\{ \frac{\partial^2 W_m}{\partial x^2} - \lambda \sum_{r=0}^m P_r W_{m-r} \right\}, \quad m = 0, 1, 2, 3, \dots \end{aligned} \quad (36)$$

Utilizing the initial condition Eq. (12), we obtain the successive solutions

$$\begin{aligned} P_0 &= \frac{1}{\left(e^{\sqrt{\frac{\lambda}{6}}x} + 1\right)^2}, \\ W_0 &= \frac{(1-\lambda)e^{\sqrt{\frac{\lambda}{6}}x} \left(e^{\sqrt{\frac{\lambda}{6}}x} + 2\right)}{\delta \left(e^{\sqrt{\frac{\lambda}{6}}x} + 1\right)^2}, \\ P_1 &= \frac{5\lambda e^{\sqrt{\frac{\lambda}{6}}x}}{3\Gamma(\mu+1) \left(e^{\sqrt{\frac{\lambda}{6}}x} + 1\right)^3}, \\ W_1 &= \frac{5\lambda(\lambda-1)e^{\sqrt{\frac{\lambda}{6}}x}}{3\delta\Gamma(\mu+1) \left(e^{\sqrt{\frac{\lambda}{6}}x} + 1\right)^3}, \\ P_2 &= \frac{25\lambda^2 e^{\sqrt{\frac{\lambda}{6}}x} \left(2e^{\sqrt{\frac{\lambda}{6}}x} - 1\right)}{18\Gamma(2\mu+1) \left(e^{\sqrt{\frac{\lambda}{6}}x} + 1\right)^4}, \\ W_2 &= \frac{25\lambda^2(\lambda-1)e^{\sqrt{\frac{\lambda}{6}}x} \left(2e^{\sqrt{\frac{\lambda}{6}}x} - 1\right)}{18\delta\Gamma(2\mu+1) \left(e^{\sqrt{\frac{\lambda}{6}}x} + 1\right)^4}, \end{aligned}$$

$$\begin{aligned}
P_3 &= -\frac{25\lambda^3\Gamma(2\mu+1)e^{\sqrt{\frac{2\lambda}{3}}x}}{9\Gamma(\mu+1)^2\Gamma(3\mu+1)\left(e^{\sqrt{\frac{\lambda}{6}}x}+1\right)^6} \\
&\quad -\frac{25\lambda^3e^{\sqrt{\frac{\lambda}{6}}x}\left(15e^{\sqrt{\frac{2\lambda}{3}}x}-20e^{\sqrt{\frac{3\lambda}{2}}x}+6e^{\sqrt{\frac{\lambda}{6}}x}-5\right)}{108\Gamma(3\mu+1)\left(e^{\sqrt{\frac{\lambda}{6}}x}+1\right)^6}, \\
W_3 &= -\frac{25\lambda^3(\lambda-1)\Gamma(2\mu+1)e^{\sqrt{\frac{2\lambda}{3}}x}}{9\delta\Gamma(\mu+1)^2\Gamma(3\mu+1)\left(e^{\sqrt{\frac{\lambda}{6}}x}+1\right)^6} \\
&\quad -\frac{25\lambda^3(\lambda-1)e^{\sqrt{\frac{\lambda}{6}}x}\left(15e^{\sqrt{\frac{2\lambda}{3}}x}-20e^{\sqrt{\frac{3\lambda}{2}}x}+6e^{\sqrt{\frac{\lambda}{6}}x}-5\right)}{108\delta\Gamma(3\mu+1)\left(e^{\sqrt{\frac{\lambda}{6}}x}+1\right)^6}, \\
P_4 &= -\frac{25\lambda^4\Gamma(2\mu+1)e^{\sqrt{\frac{2\lambda}{3}}x}\left(11e^{\sqrt{\frac{2\lambda}{3}}x}-5e^{\sqrt{\frac{\lambda}{6}}x}-1\right)}{27\Gamma(\mu+1)^2\Gamma(4\mu+1)\left(e^{\sqrt{\frac{\lambda}{6}}x}+1\right)^8} \\
&\quad -\frac{125\lambda^4\Gamma(3\mu+1)e^{\sqrt{\frac{2\lambda}{3}}x}\left(2e^{\sqrt{\frac{\lambda}{6}}x}-1\right)}{27\Gamma(\mu+1)\Gamma(2\mu+1)\Gamma(4\mu+1)\left(e^{\sqrt{\frac{\lambda}{6}}x}+1\right)^7} \\
&\quad +\frac{25\lambda^4e^{\sqrt{\frac{2\lambda}{3}}x}\left(124e^{\sqrt{\frac{2\lambda}{3}}x}+100e^{2\sqrt{\frac{2\lambda}{3}}x}+85e^{\sqrt{\frac{\lambda}{6}}x}-4\right)}{324\Gamma(4\mu+1)\left(e^{\sqrt{\frac{\lambda}{6}}x}+1\right)^8} \\
&\quad -\frac{625\lambda^4e^{\sqrt{\frac{\lambda}{6}}x}\left(17e^{2\sqrt{\frac{2\lambda}{3}}x}+1\right)}{648\Gamma(4\mu+1)\left(e^{\sqrt{\frac{\lambda}{6}}x}+1\right)^8}, \\
W_4 &= -\frac{25\lambda^4(\lambda-1)\Gamma(2\mu+1)e^{\sqrt{\frac{2\lambda}{3}}x}\left(11e^{\sqrt{\frac{2\lambda}{3}}x}-5e^{\sqrt{\frac{\lambda}{6}}x}-1\right)}{278\Gamma(\mu+1)^2\Gamma(4\mu+1)\left(e^{\sqrt{\frac{\lambda}{6}}x}+1\right)^8} \\
&\quad -\frac{125\lambda^4(\lambda-1)\Gamma(3\mu+1)e^{\sqrt{\frac{2\lambda}{3}}x}\left(2e^{\sqrt{\frac{\lambda}{6}}x}-1\right)}{278\Gamma(\mu+1)\Gamma(2\mu+1)\Gamma(4\mu+1)\left(e^{\sqrt{\frac{\lambda}{6}}x}+1\right)^7} \\
&\quad +\frac{25\lambda^4(\lambda-1)e^{\sqrt{\frac{2\lambda}{3}}x}\left(124e^{\sqrt{\frac{2\lambda}{3}}x}+100e^{2\sqrt{\frac{2\lambda}{3}}x}+85e^{\sqrt{\frac{\lambda}{6}}x}-4\right)}{324\delta\Gamma(4\mu+1)\left(e^{\sqrt{\frac{\lambda}{6}}x}+1\right)^8} \\
&\quad -\frac{625\lambda^4(\lambda-1)e^{\sqrt{\frac{\lambda}{6}}x}\left(17e^{2\sqrt{\frac{2\lambda}{3}}x}+1\right)}{648\delta\Gamma(4\mu+1)\left(e^{\sqrt{\frac{\lambda}{6}}x}+1\right)^8}.
\end{aligned}$$

Similar expression for $P_m(x, t)$ and $W_m(x, t)$, respectively, for $m = 5, 6, 7, \dots$ can be achieved. Then for system of Eq. (32), the FRDTM series solution is presented by Eq. (13).

q-HATM solution

From Eq. (27) with $\gamma = \beta = 0$, we have

$$\begin{aligned} p_m(x, t) &= (\hbar + \chi_m^*) p_{m-1} - \hbar \left(1 - \frac{\chi_m^*}{n} \right) \mathcal{L}^{-1} \left[\frac{1}{s} \left\{ g_1(x) \right\} \right] \\ &\quad - \hbar \mathcal{L}^{-1} \left[\frac{1}{s^\mu} \mathcal{L} \left[\frac{\partial^2 p_{m-1}}{\partial x^2} + p_{m-1} - \sum_{r=0}^{m-1} p_r p_{(m-1-r)} - \delta \sum_{r=0}^{m-1} p_r w_{(m-1-r)} \right] \right], \\ w_m(x, t) &= (\hbar + \chi_m^*) w_{m-1} - \hbar \left(1 - \frac{\chi_m^*}{n} \right) \mathcal{L}^{-1} \left[\frac{1}{s} \left\{ g_2(x) \right\} \right] \\ &\quad - \hbar \mathcal{L}^{-1} \left[\frac{1}{s^\mu} \mathcal{L} \left[\frac{\partial^2 w_{m-1}}{\partial x^2} - \lambda \sum_{r=0}^{m-1} p_r w_{(m-1-r)} \right] \right], \quad m = 1, 2, 3, \dots \end{aligned} \quad (37)$$

On solving Eq. (37) with the aid of Eq. (26), we get the iterative terms of p and w as follows:

$$\begin{aligned} p_0 &= \frac{1}{\left(e^{\sqrt{\frac{\lambda}{6}}x} + 1 \right)^2}, \\ w_0 &= \frac{(1-\lambda)e^{\sqrt{\frac{\lambda}{6}}x} \left(e^{\sqrt{\frac{\lambda}{6}}x} + 2 \right)}{\delta \left(e^{\sqrt{\frac{\lambda}{6}}x} + 1 \right)^2}, \\ p_1 &= -\frac{5\hbar\lambda e^{\sqrt{\frac{\lambda}{6}}x}}{3\Gamma(\mu+1) \left(e^{\sqrt{\frac{\lambda}{6}}x} + 1 \right)^3} t^\mu, \\ w_1 &= -\frac{5\hbar\lambda(\lambda-1)e^{\sqrt{\frac{\lambda}{6}}x}}{3\delta\Gamma(\mu+1) \left(e^{\sqrt{\frac{\lambda}{6}}x} + 1 \right)^3} t^\mu, \\ p_2 &= (\hbar+n)p_1 + \frac{25\hbar^2\lambda^2 e^{\sqrt{\frac{\lambda}{6}}x} \left(2e^{\sqrt{\frac{\lambda}{6}}x} - 1 \right)}{18\Gamma(2\mu+1) \left(e^{\sqrt{\frac{\lambda}{6}}x} + 1 \right)^4} t^{2\mu}, \\ w_2 &= (\hbar+n)w_1 + \frac{25\hbar^2\lambda^2(\lambda-1)e^{\sqrt{\frac{\lambda}{6}}x} \left(2e^{\sqrt{\frac{\lambda}{6}}x} - 1 \right)}{18\delta\Gamma(2\mu+1) \left(e^{\sqrt{\frac{\lambda}{6}}x} + 1 \right)^4} t^{2\mu}, \\ p_3 &= (\hbar+n)p_2 + \frac{25\hbar^2(\hbar+n)\lambda^2 e^{\sqrt{\frac{\lambda}{6}}x} \left(2e^{\sqrt{\frac{\lambda}{6}}x} - 1 \right)}{18\Gamma(2\mu+1) \left(e^{\sqrt{\frac{\lambda}{6}}x} + 1 \right)^4} t^{2\mu} \end{aligned}$$

$$\begin{aligned}
& + \frac{25\hbar^3\lambda^3\Gamma(2\mu+1)e^{\sqrt{\frac{2\lambda}{3}}x}}{9\Gamma(\mu+1)^2\Gamma(3\mu+1)\left(e^{\sqrt{\frac{2\lambda}{3}}x}+1\right)^6}t^{3\mu} \\
& + \frac{25\hbar^3\lambda^3e^{\sqrt{\frac{\lambda}{6}}x}\left(15e^{\sqrt{\frac{2\lambda}{3}}x}-20e^{\sqrt{\frac{3\lambda}{2}}x}+6e^{\sqrt{\frac{\lambda}{6}}x}-5\right)}{108\Gamma(3\mu+1)\left(e^{\sqrt{\frac{\lambda}{6}}x}+1\right)^6}t^{3\mu}, \\
w_3 = (\hbar+n)w_2 & + \frac{25\hbar^2\lambda^2(\hbar+n)(\lambda-1)e^{\sqrt{\frac{\lambda}{6}}x}\left(2e^{\sqrt{\frac{\lambda}{6}}x}-1\right)}{18\delta\Gamma(2\mu+1)\left(e^{\sqrt{\frac{\lambda}{6}}x}+1\right)^4}t^{2\mu} \\
& + \frac{25\hbar^3\lambda^3(\lambda-1)\Gamma(2\mu+1)e^{\sqrt{\frac{2\lambda}{3}}x}}{9\delta\Gamma(\mu+1)^2\Gamma(3\mu+1)\left(e^{\sqrt{\frac{2\lambda}{3}}x}+1\right)^6}t^{3\mu} \\
& + \frac{25\hbar^3\lambda^3(\lambda-1)e^{\sqrt{\frac{\lambda}{6}}x}\left(15e^{\sqrt{\frac{2\lambda}{3}}x}-20e^{\sqrt{\frac{3\lambda}{2}}x}+6e^{\sqrt{\frac{\lambda}{6}}x}-5\right)}{108\delta\Gamma(3\mu+1)\left(e^{\sqrt{\frac{\lambda}{6}}x}+1\right)^6}t^{3\mu}, \\
p_4 = (\hbar+n)p_3 & + \frac{25\hbar^2(\hbar+n)^2\lambda^2e^{\sqrt{\frac{\lambda}{6}}x}\left(2e^{\sqrt{\frac{\lambda}{6}}x}-1\right)}{18\Gamma(2\mu+1)\left(e^{\sqrt{\frac{\lambda}{6}}x}+1\right)^4}t^{2\mu} \\
& + \frac{25(\hbar+n)\hbar^3\lambda^3\Gamma(2\mu+1)e^{\sqrt{\frac{2\lambda}{3}}x}}{9\Gamma(\mu+1)^2\Gamma(3\mu+1)\left(e^{\sqrt{\frac{2\lambda}{3}}x}+1\right)^6}t^{3\mu} \\
& + \frac{25(\hbar+n)\hbar^3\lambda^3e^{\sqrt{\frac{\lambda}{6}}x}\left(15e^{\sqrt{\frac{2\lambda}{3}}x}-20e^{\sqrt{\frac{3\lambda}{2}}x}+6e^{\sqrt{\frac{\lambda}{6}}x}-5\right)}{108\Gamma(3\mu+1)\left(e^{\sqrt{\frac{\lambda}{6}}x}+1\right)^6}t^{3\mu} \\
& - \frac{625\hbar^4\lambda^4e^{\sqrt{\frac{\lambda}{6}}x}\left(17e^{2\sqrt{\frac{2\lambda}{3}}x}+1\right)}{648\Gamma(4\mu+1)\left(e^{\sqrt{\frac{2\lambda}{3}}x}+1\right)^8}t^{4\mu} \\
& - \frac{25\hbar^4\lambda^4\Gamma(2\mu+1)e^{\sqrt{\frac{2\lambda}{3}}x}\left(11e^{\sqrt{\frac{2\lambda}{3}}x}-5e^{\sqrt{\frac{\lambda}{6}}x}-1\right)}{27\Gamma(\mu+1)^2\Gamma(4\mu+1)\left(e^{\sqrt{\frac{\lambda}{6}}x}+1\right)^8}t^{4\mu} \\
& - \frac{125\hbar^4\lambda^4\Gamma(3\mu+1)e^{\sqrt{\frac{2\lambda}{3}}x}\left(2e^{\sqrt{\frac{\lambda}{6}}x}-1\right)}{27\Gamma(\mu+1)\Gamma(2\mu+1)\Gamma(4\mu+1)\left(e^{\sqrt{\frac{\lambda}{6}}x}+1\right)^7}t^{4\mu} \\
& + \frac{25\hbar^4\lambda^4e^{\sqrt{\frac{2\lambda}{3}}x}\left(124e^{\sqrt{\frac{2\lambda}{3}}x}+100e^{2\sqrt{\frac{2\lambda}{3}}x}+85e^{\sqrt{\frac{\lambda}{6}}x}-4\right)}{324\Gamma(4\mu+1)\left(e^{\sqrt{\frac{\lambda}{6}}x}+1\right)^8}t^{4\mu},
\end{aligned}$$

$$\begin{aligned}
w_4 = & (\hbar + n) w_3 + \frac{25(\hbar + n)^2 \hbar^2 \lambda^2 (\lambda - 1) e^{\sqrt{\frac{\lambda}{6}}x} \left(2e^{\sqrt{\frac{\lambda}{6}}x} - 1 \right)}{188\delta\Gamma(2\mu + 1) \left(e^{\sqrt{\frac{\lambda}{6}}x} + 1 \right)^4} t^{2\mu} \\
& + \frac{25(\hbar + n) \hbar^3 \lambda^3 (\lambda - 1) \Gamma(2\mu + 1) e^{\sqrt{\frac{2\lambda}{3}}x}}{98\Gamma(\mu + 1)^2 \Gamma(3\mu + 1) \left(e^{\sqrt{\frac{\lambda}{6}}x} + 1 \right)^6} t^{3\mu} \\
& + \frac{25(\hbar + n) \hbar^3 \lambda^3 (\lambda - 1) e^{\sqrt{\frac{\lambda}{6}}x} \left(15e^{\sqrt{\frac{2\lambda}{3}}x} - 20e^{\sqrt{\frac{3\lambda}{2}}x} + 6e^{\sqrt{\frac{\lambda}{6}}x} - 5 \right)}{108\delta\Gamma(3\mu + 1) \left(e^{\sqrt{\frac{\lambda}{6}}x} + 1 \right)^6} t^{3\mu} \\
& - \frac{625\hbar^4 \lambda^4 (\lambda - 1) e^{\sqrt{\frac{\lambda}{6}}x} \left(17e^{2\sqrt{\frac{2\lambda}{3}}x} + 1 \right)}{648\delta\Gamma(4\mu + 1) \left(e^{\sqrt{\frac{\lambda}{6}}x} + 1 \right)^8} t^{4\mu} \\
& - \frac{25\hbar^4 \lambda^4 (\lambda - 1) \Gamma(2\mu + 1) e^{\sqrt{\frac{2\lambda}{3}}x} \left(11e^{\sqrt{\frac{2\lambda}{3}}x} - 5e^{\sqrt{\frac{\lambda}{6}}x} - 1 \right)}{278\Gamma(\mu + 1)^2 \Gamma(4\mu + 1) \left(e^{\sqrt{\frac{\lambda}{6}}x} + 1 \right)^8} t^{4\mu} \\
& - \frac{125\hbar^4 \lambda^4 (\lambda - 1) \Gamma(3\mu + 1) e^{\sqrt{\frac{2\lambda}{3}}x} \left(2e^{\sqrt{\frac{\lambda}{6}}x} - 1 \right)}{278\Gamma(\mu + 1) \Gamma(2\mu + 1) \Gamma(4\mu + 1) \left(e^{\sqrt{\frac{\lambda}{6}}x} + 1 \right)^7} t^{4\mu} \\
& + \frac{25\hbar^4 \lambda^4 (\lambda - 1) e^{\sqrt{\frac{2\lambda}{3}}x} \left(124e^{\sqrt{\frac{2\lambda}{3}}x} + 100e^{2\sqrt{\frac{2\lambda}{3}}x} + 85e^{\sqrt{\frac{\lambda}{6}}x} - 4 \right)}{3248\delta\Gamma(4\mu + 1) \left(e^{\sqrt{\frac{\lambda}{6}}x} + 1 \right)^8} t^{4\mu}.
\end{aligned}$$

Similar expression for p_m and w_m , respectively, for $m = 5, 6, 7, \dots$ can be achieved. Then, for system of Eq. (32), the q-HATM series solution is presented by Eq. (28).

Case 2 Consider the nonlinear TFB-Z system at $\gamma = \lambda$ and $\beta = 1$, then Eq. (7) reduced to

$$\begin{aligned}
\mathcal{D}_t^\mu p &= \frac{\partial^2 p}{\partial x^2} + \delta w + p - p^2 - \delta pw, \quad 0 < \mu \leq 1, \\
\mathcal{D}_t^\mu w &= \frac{\partial^2 w}{\partial x^2} + \lambda w - \lambda pw,
\end{aligned} \tag{38}$$

with the initial condition

$$\begin{aligned}
p(x, 0) &= \frac{1}{\left(e^{\sqrt{\frac{\lambda}{6}}x} + 1 \right)^2}, \\
w(x, 0) &= \frac{\lambda - 1}{\delta \left(e^{\sqrt{\frac{\lambda}{6}}x} + 1 \right)^2}.
\end{aligned} \tag{39}$$

The exact solution of Eq. (38) when $\mu = 1$ is

$$\begin{aligned} p(x, t) &= \frac{e^{\frac{5\lambda}{3}t}}{\left(e^{\sqrt{\frac{\lambda}{6}}x} + e^{\frac{5\lambda}{6}t}\right)^2}, \\ w(x, t) &= \frac{(\lambda - 1)e^{\frac{5\lambda}{3}t}}{\delta\left(e^{\sqrt{\frac{\lambda}{6}}x} + e^{\frac{5\lambda}{6}t}\right)^2}, \end{aligned} \quad (40)$$

where $\lambda \neq 1$ is a positive parameter.

Remark 2 The exact solution can also have the following form:

$$\begin{aligned} \frac{e^{\frac{5\lambda}{3}t}}{\left(e^{\sqrt{\frac{\lambda}{6}}x} + e^{\frac{5\lambda}{6}t}\right)^2} &= \frac{1}{4} \left(\tanh \left(\sqrt{\frac{\lambda}{24}}x - \frac{5\lambda}{12}t \right) - 1 \right)^2, \\ \frac{(\lambda - 1)e^{\frac{5\lambda}{3}t}}{\delta\left(e^{\sqrt{\frac{\lambda}{6}}x} + e^{\frac{5\lambda}{6}t}\right)^2} &= \frac{\lambda - 1}{4\delta} \left(\tanh \left(\sqrt{\frac{\lambda}{24}}x - \frac{5\lambda}{12}t \right) - 1 \right)^2. \end{aligned} \quad (41)$$

FRDTM solution

From Eq. (11) with $\gamma = \lambda$ and $\beta = 1$, we have

$$\begin{aligned} P_{(m+1)}(x) &= \frac{\Gamma(m\mu + 1)}{\Gamma(m\mu + \mu + 1)} \left\{ \frac{\partial^2 P_m}{\partial x^2} + \delta W_m + P_m - \sum_{r=0}^m P_r P_{m-r} - \delta \sum_{r=0}^m P_r W_{m-r} \right\}, \\ W_{(m+1)}(x) &= \frac{\Gamma(m\mu + 1)}{\Gamma(m\mu + \mu + 1)} \left\{ \frac{\partial^2 W_m}{\partial x^2} + \lambda W_m - \lambda \sum_{r=0}^m P_r W_{m-r} \right\}, \quad m = 0, 1, 2, 3, \dots \end{aligned} \quad (42)$$

Using the initial condition Eq. (12), we obtain the successive solutions

$$\begin{aligned} P_0 &= \frac{1}{\left(e^{\sqrt{\frac{\lambda}{6}}x} + 1\right)^2}, \\ W_0 &= \frac{\lambda - 1}{\delta\left(e^{\sqrt{\frac{\lambda}{6}}x} + 1\right)^2}, \\ P_1 &= \frac{5\lambda e^{\sqrt{\frac{\lambda}{6}}x}}{3\Gamma(\mu + 1)\left(e^{\sqrt{\frac{\lambda}{6}}x} + 1\right)^3}, \\ W_1 &= \frac{5\lambda(\lambda - 1)e^{\sqrt{\frac{\lambda}{6}}x}}{3\delta\Gamma(\mu + 1)\left(e^{\sqrt{\frac{\lambda}{6}}x} + 1\right)^3}, \end{aligned}$$

$$\begin{aligned}
P_2 &= \frac{25\lambda^2 e^{\sqrt{\frac{\lambda}{6}}x} (2e^{\sqrt{\frac{\lambda}{6}}x} - 1)}{18\Gamma(2\mu + 1) (e^{\sqrt{\frac{\lambda}{6}}x} + 1)^4}, \\
W_2 &= \frac{25\lambda^2(\lambda - 1)e^{\sqrt{\frac{\lambda}{6}}x} (2e^{\sqrt{\frac{\lambda}{6}}x} - 1)}{18\delta\Gamma(2\mu + 1) (e^{\sqrt{\frac{\lambda}{6}}x} + 1)^4}, \\
P_3 &= -\frac{25\lambda^3\Gamma(2\mu + 1)e^{\sqrt{\frac{2\lambda}{3}}x}}{9\Gamma(\mu + 1)^2\Gamma(3\mu + 1) (e^{\sqrt{\frac{\lambda}{6}}x} + 1)^6} \\
&\quad - \frac{25\lambda^3 e^{\sqrt{\frac{\lambda}{6}}x} (15e^{\sqrt{\frac{2\lambda}{3}}x} - 20e^{\sqrt{\frac{3\lambda}{2}}x} + 6e^{\sqrt{\frac{\lambda}{6}}x} - 5)}{108\Gamma(3\mu + 1) (e^{\sqrt{\frac{\lambda}{6}}x} + 1)^6}, \\
W_3 &= -\frac{25(\lambda - 1)\lambda^3\Gamma(2\mu + 1)e^{\sqrt{\frac{2\lambda}{3}}x}}{9\delta\Gamma(\mu + 1)^2\Gamma(3\mu + 1) (e^{\sqrt{\frac{\lambda}{6}}x} + 1)^6} \\
&\quad - \frac{25(\lambda - 1)\lambda^3 e^{\sqrt{\frac{\lambda}{6}}x} (15e^{\sqrt{\frac{2\lambda}{3}}x} - 20e^{\sqrt{\frac{3\lambda}{2}}x} + 6e^{\sqrt{\frac{\lambda}{6}}x} - 5)}{108\delta\Gamma(3\mu + 1) (e^{\sqrt{\frac{\lambda}{6}}x} + 1)^6}, \\
P_4 &= -\frac{25\lambda^4\Gamma(2\mu + 1)e^{\sqrt{\frac{2\lambda}{3}}x} (11e^{\sqrt{\frac{2\lambda}{3}}x} - 5e^{\sqrt{\frac{\lambda}{6}}x} - 1)}{27\Gamma(\mu + 1)^2\Gamma(4\mu + 1) (e^{\sqrt{\frac{\lambda}{6}}x} + 1)^8} \\
&\quad - \frac{125\lambda^4\Gamma(3\mu + 1)e^{\sqrt{\frac{2\lambda}{3}}x} (2e^{\sqrt{\frac{\lambda}{6}}x} - 1)}{27\Gamma(\mu + 1)\Gamma(2\mu + 1)\Gamma(4\mu + 1) (e^{\sqrt{\frac{\lambda}{6}}x} + 1)^7} \\
&\quad + \frac{25\lambda^4 e^{\sqrt{\frac{2\lambda}{3}}x} (124e^{\sqrt{\frac{2\lambda}{3}}x} + 100e^{2\sqrt{\frac{2\lambda}{3}}x} + 85e^{\sqrt{\frac{\lambda}{6}}x} - 4)}{324\Gamma(4\mu + 1) (e^{\sqrt{\frac{\lambda}{6}}x} + 1)^8} \\
&\quad - \frac{625\lambda^4 e^{\sqrt{\frac{\lambda}{6}}x} (17e^{2\sqrt{\frac{2\lambda}{3}}x} + 1)}{648\Gamma(4\mu + 1) (e^{\sqrt{\frac{\lambda}{6}}x} + 1)^8}, \\
W_4 &= -\frac{25\lambda^4(\lambda - 1)\Gamma(2\mu + 1)e^{\sqrt{\frac{2\lambda}{3}}x} (11e^{\sqrt{\frac{2\lambda}{3}}x} - 5e^{\sqrt{\frac{\lambda}{6}}x} - 1)}{278\Gamma(\mu + 1)^2\Gamma(4\mu + 1) (e^{\sqrt{\frac{\lambda}{6}}x} + 1)^8} \\
&\quad - \frac{125\lambda^4(\lambda - 1)\Gamma(3\mu + 1)e^{\sqrt{\frac{2\lambda}{3}}x} (2e^{\sqrt{\frac{\lambda}{6}}x} - 1)}{278\Gamma(\mu + 1)\Gamma(2\mu + 1)\Gamma(4\mu + 1) (e^{\sqrt{\frac{\lambda}{6}}x} + 1)^7}
\end{aligned}$$

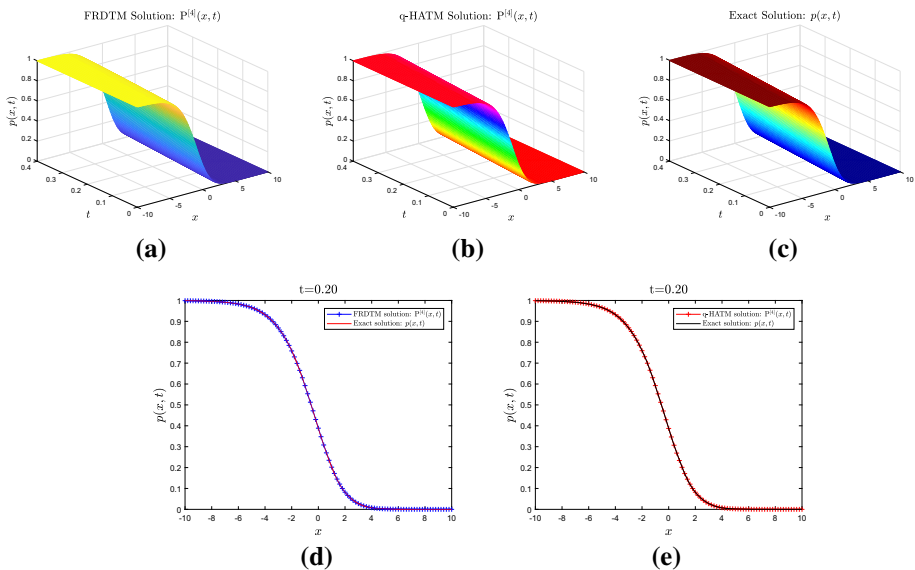


Fig. 1 The 3D and 2D comparison of FRDTM, q-HATM ($n = 1, \hbar = -1$) and exact solution for $p(x, t)$ in a–e when $\mu = 1, \delta = 2$ and $\lambda = 3$ for Case 1

$$\begin{aligned}
 & + \frac{25\lambda^4(\lambda-1)e^{\sqrt{\frac{2\lambda}{3}}x} \left(124e^{\sqrt{\frac{2\lambda}{3}}x} + 100e^{2\sqrt{\frac{2\lambda}{3}}x} + 85e^{\sqrt{\frac{\lambda}{6}}x} - 4 \right)}{324\delta\Gamma(4\mu+1)\left(e^{\sqrt{\frac{\lambda}{6}}x} + 1\right)^8} \\
 & - \frac{625\lambda^4(\lambda-1)e^{\sqrt{\frac{\lambda}{6}}x} \left(17e^{2\sqrt{\frac{2\lambda}{3}}x} + 1 \right)}{648\delta\Gamma(4\mu+1)\left(e^{\sqrt{\frac{\lambda}{6}}x} + 1\right)^8}.
 \end{aligned}$$

Similar expression for P_m and W_m , respectively, for $m = 5, 6, 7, \dots$ can be achieved. Then for system of Eq. (38) with initial condition Eq. (39), the FRDTM series solution is presented by Eq. (13).

q-HATM solution

From Eq. (27) with $\gamma = \lambda$ and $\beta = 1$, we have

$$\begin{aligned}
 p_m(x, t) = & (\hbar + \chi_m^*) p_{m-1} - \hbar \left(1 - \frac{\chi_m^*}{n} \right) \mathcal{L}^{-1} \left[\frac{1}{s} \left\{ g_1(x) \right\} \right] - \hbar \mathcal{L}^{-1} \left[\frac{1}{s^\mu} \mathcal{L} \left[\frac{\partial^2 p_{m-1}}{\partial x^2} \right. \right. \\
 & \left. \left. + \delta w_{m-1} + p_{m-1} - \sum_{r=0}^{m-1} p_r p_{(m-1-r)} - \delta \sum_{r=0}^{m-1} p_r w_{(m-1-r)} \right] \right],
 \end{aligned}$$

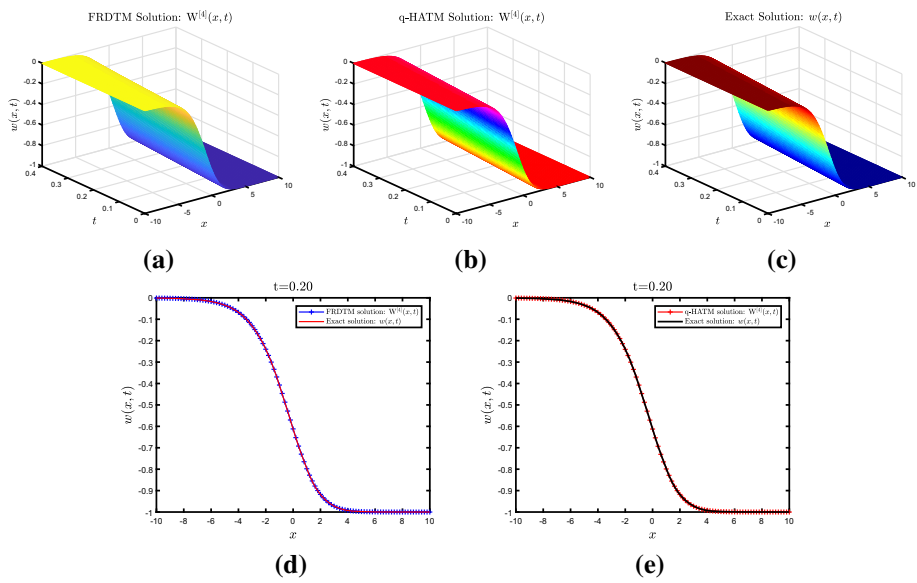


Fig. 2 The 3D and 2D comparison of FRDTM, q-HATM ($n = 1, \hbar = -1$) and exact solution for $w(x, t)$ in a–e when $\mu = 1, \delta = 2$ and $\lambda = 3$ for Case 1

$$\begin{aligned}
 w_m(x, t) &= (\hbar + \chi_m^*) w_{m-1} - \hbar \left(1 - \frac{\chi_m^*}{n} \right) \mathcal{L}^{-1} \left[\frac{1}{s} \left\{ g_2(x) \right\} \right] \\
 &\quad - \hbar \mathcal{L}^{-1} \left[\frac{1}{s^\mu} \mathcal{L} \left[\frac{\partial^2 w_{m-1}}{\partial x^2} + \lambda w_{m-1} - \lambda \sum_{r=0}^{m-1} p_r w_{(m-1-r)} \right] \right], \quad m = 1, 2, 3, \dots
 \end{aligned} \tag{43}$$

On solving Eq. (43) with the aid of Eq. (26), we get the iterative terms of p and w as follows:

$$\begin{aligned}
 p_0 &= \frac{1}{\left(e^{\sqrt{\frac{\lambda}{6}}x} + 1 \right)^2}, \\
 w_0 &= \frac{\lambda - 1}{\delta \left(e^{\sqrt{\frac{\lambda}{6}}x} + 1 \right)^2}, \\
 p_1 &= - \frac{5\hbar\lambda e^{\sqrt{\frac{\lambda}{6}}x}}{3\Gamma(\mu + 1) \left(e^{\sqrt{\frac{\lambda}{6}}x} + 1 \right)^3} t^\mu, \\
 w_1 &= - \frac{5\hbar\lambda(\lambda - 1) e^{\sqrt{\frac{\lambda}{6}}x}}{3\delta\Gamma(\mu + 1) \left(e^{\sqrt{\frac{\lambda}{6}}x} + 1 \right)^3} t^\mu, \\
 p_2 &= (\hbar + n)p_1 + \frac{25\hbar^2\lambda^2 e^{\sqrt{\frac{\lambda}{6}}x} \left(2e^{\sqrt{\frac{\lambda}{6}}x} - 1 \right)}{18\Gamma(2\mu + 1) \left(e^{\sqrt{\frac{\lambda}{6}}x} + 1 \right)^4} t^{2\mu},
 \end{aligned}$$

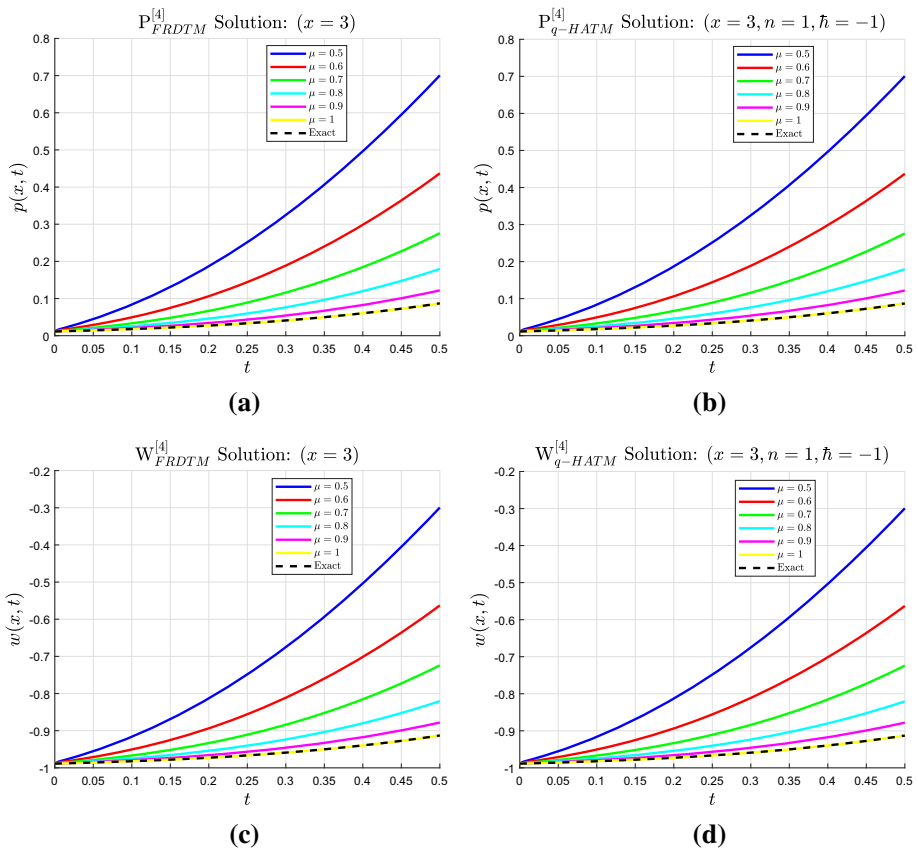


Fig. 3 Solution profiles in **a-d** with different μ values when $x = 3$, $\delta = 2$ and $\lambda = 3$ for Case 1

$$w_2 = (\hbar + n) w_1 + \frac{25\hbar^2\lambda^2(\lambda - 1)e^{\sqrt{\frac{\lambda}{6}}x}\left(2e^{\sqrt{\frac{\lambda}{6}}x} - 1\right)}{18\delta\Gamma(2\mu + 1)\left(e^{\sqrt{\frac{\lambda}{6}}x} + 1\right)^4}t^{2\mu},$$

$$p_3 = (\hbar + n) p_2 + \frac{25\hbar^2(\hbar + n)\lambda^2 e^{\sqrt{\frac{\lambda}{6}}x}\left(2e^{\sqrt{\frac{\lambda}{6}}x} - 1\right)}{18\Gamma(2\mu + 1)\left(e^{\sqrt{\frac{\lambda}{6}}x} + 1\right)^4}t^{2\mu}$$

$$+ \frac{25\hbar^3\lambda^3\Gamma(2\mu + 1)e^{\sqrt{\frac{2\lambda}{3}}x}}{9\Gamma(\mu + 1)^2\Gamma(3\mu + 1)\left(e^{\sqrt{\frac{\lambda}{6}}x} + 1\right)^6}t^{3\mu}$$

$$+ \frac{25\hbar^3\lambda^3e^{\sqrt{\frac{\lambda}{6}}x}\left(15e^{\sqrt{\frac{2\lambda}{3}}x} - 20e^{\sqrt{\frac{3\lambda}{2}}x} + 6e^{\sqrt{\frac{\lambda}{6}}x} - 5\right)}{108\Gamma(3\mu + 1)\left(e^{\sqrt{\frac{\lambda}{6}}x} + 1\right)^6}t^{3\mu},$$

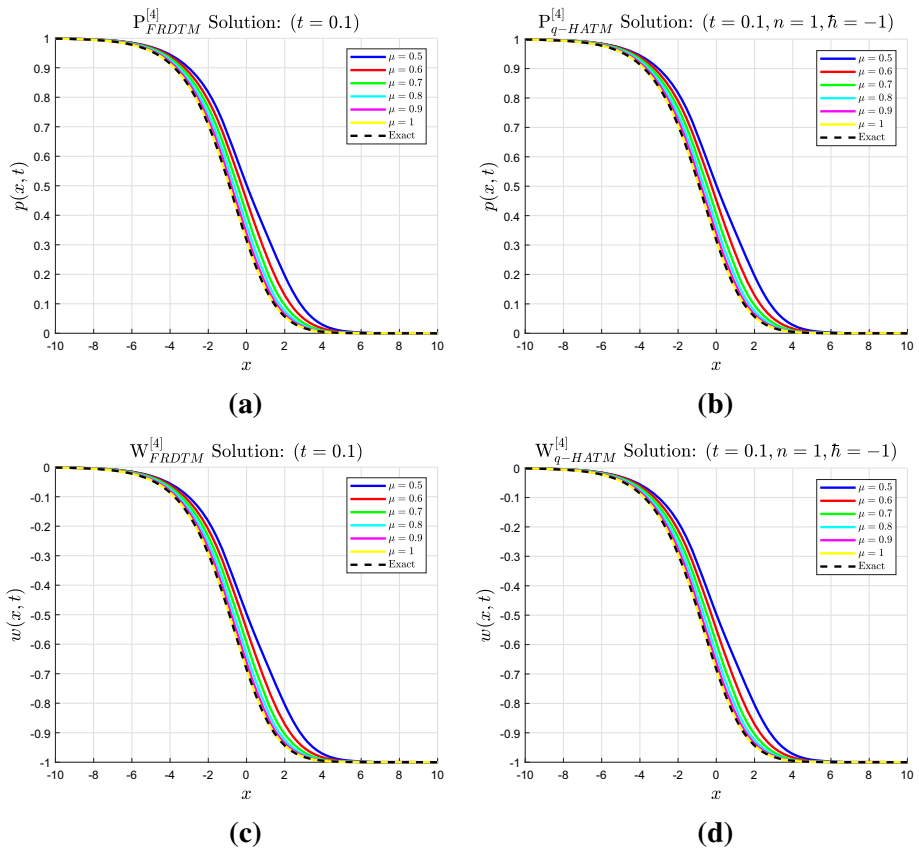


Fig. 4 Solution profiles in a–d with different μ values when $t = 0.1$, $\delta = 2$ and $\lambda = 3$ for Case 1

$$\begin{aligned}
 w_3 &= (\hbar + n)w_2 + \frac{25\hbar^2\lambda^2(\hbar + n)(\lambda - 1)e^{\sqrt{\frac{\lambda}{6}}x}\left(2e^{\sqrt{\frac{\lambda}{6}}x} - 1\right)}{188\Gamma(2\mu + 1)\left(e^{\sqrt{\frac{\lambda}{6}}x} + 1\right)^4}t^{2\mu} \\
 &\quad + \frac{25\hbar^3\lambda^3(\lambda - 1)\Gamma(2\mu + 1)e^{\sqrt{\frac{2\lambda}{3}}x}}{9\delta\Gamma(\mu + 1)^2\Gamma(3\mu + 1)\left(e^{\sqrt{\frac{\lambda}{6}}x} + 1\right)^6}t^{3\mu} \\
 &\quad + \frac{25\hbar^3\lambda^3(\lambda - 1)e^{\sqrt{\frac{\lambda}{6}}x}\left(15e^{\sqrt{\frac{2\lambda}{3}}x} - 20e^{\sqrt{\frac{3\lambda}{2}}x} + 6e^{\sqrt{\frac{\lambda}{6}}x} - 5\right)}{108\delta\Gamma(3\mu + 1)\left(e^{\sqrt{\frac{\lambda}{6}}x} + 1\right)^6}t^{3\mu}, \\
 p_4 &= (\hbar + n)p_3 + \frac{25\hbar^2(\hbar + n)^2\lambda^2e^{\sqrt{\frac{\lambda}{6}}x}\left(2e^{\sqrt{\frac{\lambda}{6}}x} - 1\right)}{18\Gamma(2\mu + 1)\left(e^{\sqrt{\frac{\lambda}{6}}x} + 1\right)^4}t^{2\mu}
 \end{aligned}$$

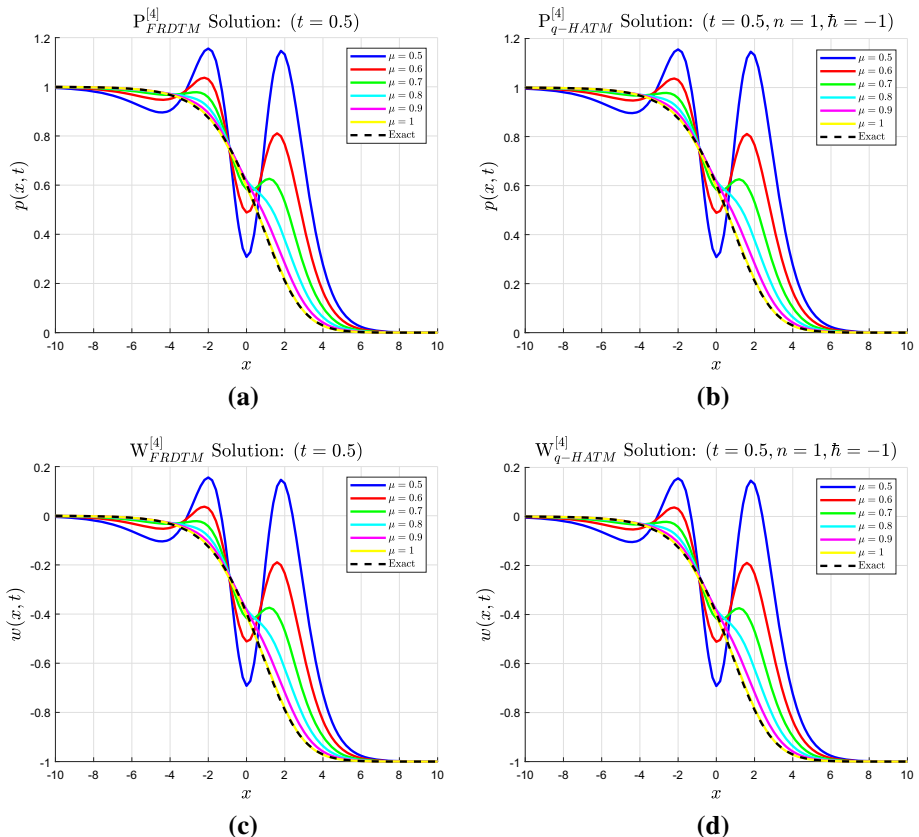


Fig. 5 Solution profiles in **a–d** with different μ values when $t = 0.5$, $\delta = 2$ and $\lambda = 3$ for Case 1

$$\begin{aligned}
 & + \frac{25(\hbar+n)\hbar^3\lambda^3\Gamma(2\mu+1)e^{\sqrt{\frac{2\lambda}{3}}x}}{9\Gamma(\mu+1)^2\Gamma(3\mu+1)(e^{\sqrt{\frac{\lambda}{6}}x}+1)^6}t^{3\mu} \\
 & + \frac{25(\hbar+n)\hbar^3\lambda^3e^{\sqrt{\frac{\lambda}{6}}x}(15e^{\sqrt{\frac{2\lambda}{3}}x}-20e^{\sqrt{\frac{3\lambda}{2}}x}+6e^{\sqrt{\frac{\lambda}{6}}x}-5)}{108\Gamma(3\mu+1)(e^{\sqrt{\frac{\lambda}{6}}x}+1)^6}t^{3\mu} \\
 & - \frac{625\hbar^4\lambda^4e^{\sqrt{\frac{\lambda}{6}}x}(17e^{2\sqrt{\frac{2\lambda}{3}}x}+1)}{648\Gamma(4\mu+1)(e^{\sqrt{\frac{\lambda}{6}}x}+1)^8}t^{4\mu} \\
 & - \frac{25\hbar^4\lambda^4\Gamma(2\mu+1)e^{\sqrt{\frac{2\lambda}{3}}x}(11e^{\sqrt{\frac{2\lambda}{3}}x}-5e^{\sqrt{\frac{\lambda}{6}}x}-1)}{27\Gamma(\mu+1)^2\Gamma(4\mu+1)(e^{\sqrt{\frac{\lambda}{6}}x}+1)^8}t^{4\mu}
 \end{aligned}$$

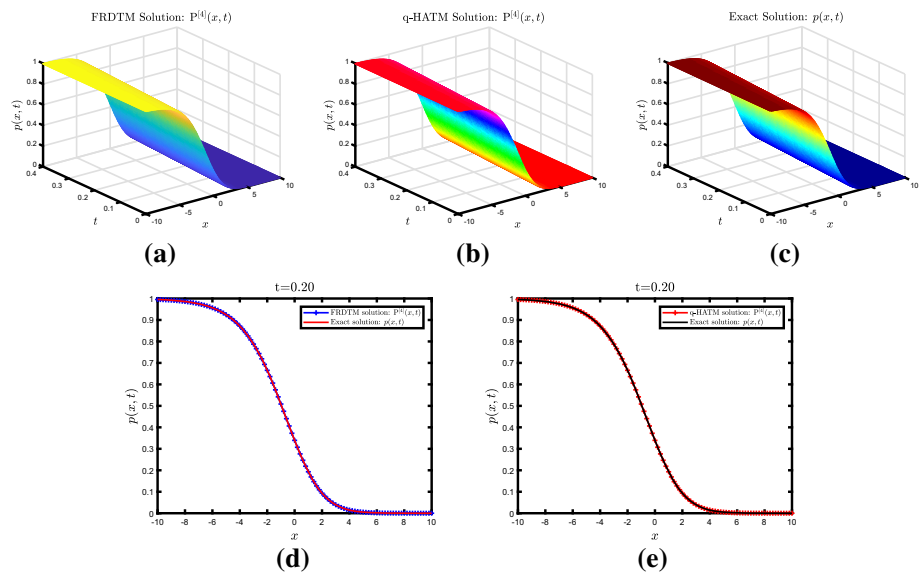


Fig. 6 The 3D and 2D comparison of FRDTM, q-HATM ($n = 1, \hbar = -1$) and exact solution for $p(x, t)$ when $\mu = 1, \delta = 2$ and $\lambda = 2$ in a–e for Case 2

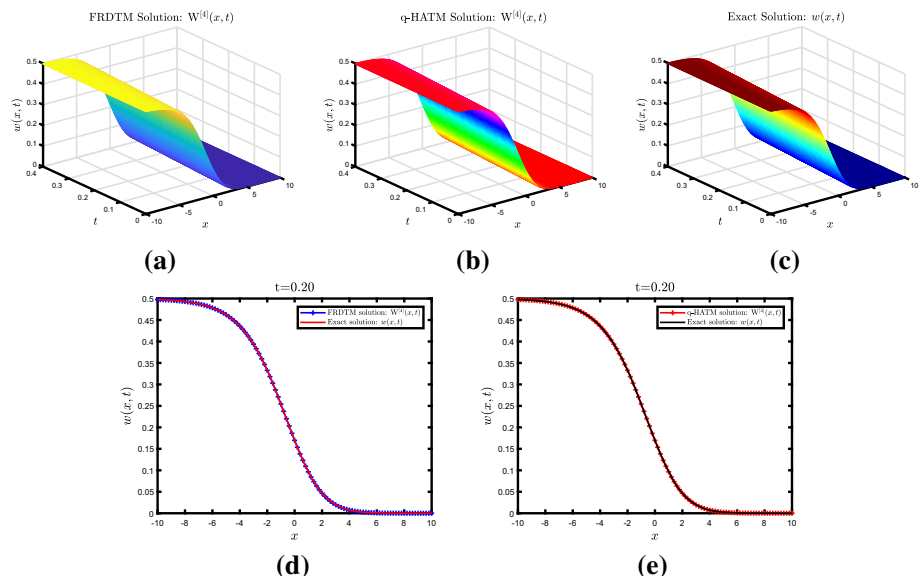


Fig. 7 The 3D and 2D comparison of FRDTM, q-HATM ($n = 1, \hbar = -1$) and exact solution for $w(x, t)$ when $\mu = 1, \delta = 2$ and $\lambda = 2$ in a–e for Case 2

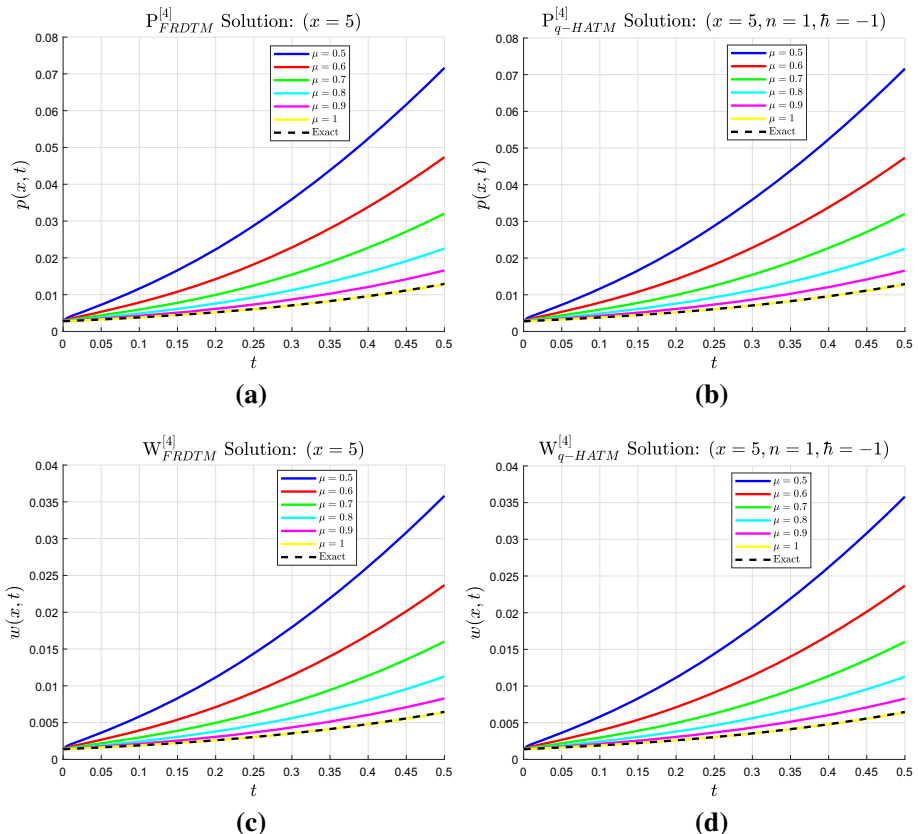


Fig. 8 Solution profiles in **a–d** with different μ values when $x = 5$, $\delta = 2$ and $\lambda = 2$ for Case 2

$$w_4 = (\hbar + n) w_3 + \frac{125\hbar^4\lambda^4\Gamma(3\mu + 1)e^{\sqrt{\frac{\lambda}{6}}x}\left(2e^{\sqrt{\frac{\lambda}{6}}x} - 1\right)}{27\Gamma(\mu + 1)\Gamma(2\mu + 1)\Gamma(4\mu + 1)\left(e^{\sqrt{\frac{\lambda}{6}}x} + 1\right)^7 t^{4\mu}} \\ + \frac{25\hbar^4\lambda^4 e^{\sqrt{\frac{2\lambda}{3}}x}\left(124e^{\sqrt{\frac{2\lambda}{3}}x} + 100e^{2\sqrt{\frac{2\lambda}{3}}x} + 85e^{\sqrt{\frac{\lambda}{6}}x} - 4\right)}{324\Gamma(4\mu + 1)\left(e^{\sqrt{\frac{\lambda}{6}}x} + 1\right)^8 t^{4\mu}},$$

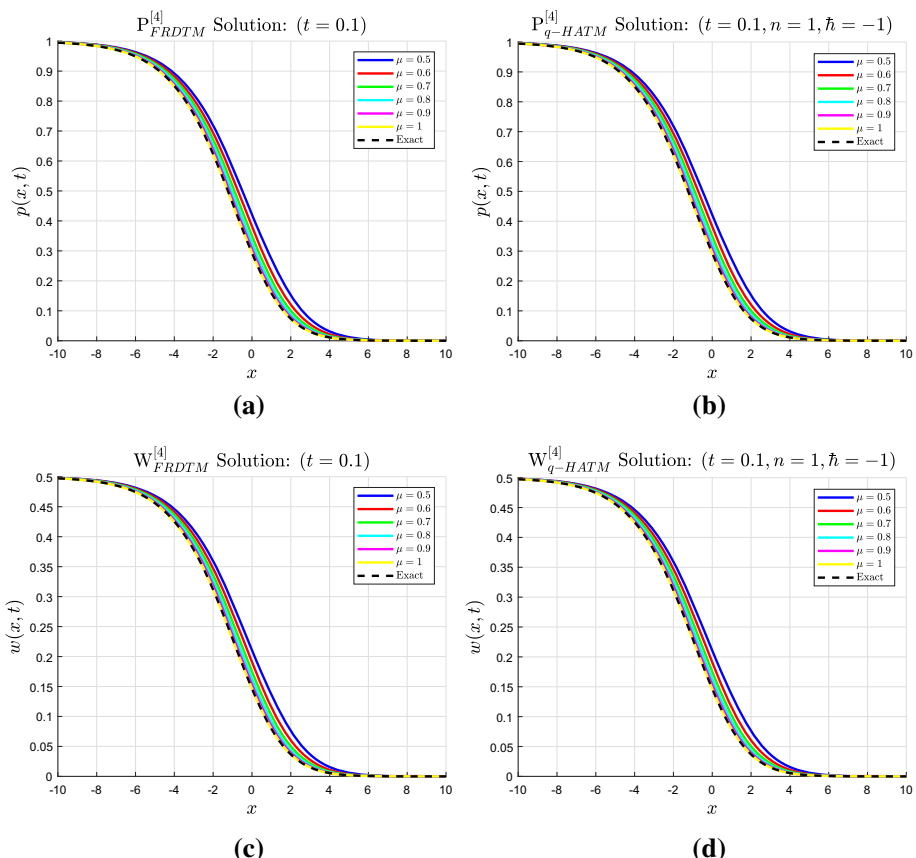


Fig. 9 Solution profiles in **a–d** with different μ values when $t = 0.1$, $\delta = 2$ and $\lambda = 2$ for Case 2

$$\begin{aligned}
& + \frac{25(\hbar+n)\hbar^3\lambda^3(\lambda-1)e^{\sqrt{\frac{\lambda}{6}}x} \left(15e^{\sqrt{\frac{2\lambda}{3}}x} - 20e^{\sqrt{\frac{3\lambda}{2}}x} + 6e^{\sqrt{\frac{\lambda}{6}}x} - 5 \right)}{1088\Gamma(3\mu+1) \left(e^{\sqrt{\frac{\lambda}{6}}x} + 1 \right)^6} t^{3\mu} \\
& - \frac{625\hbar^4\lambda^4(\lambda-1)e^{\sqrt{\frac{\lambda}{6}}x} \left(17e^{2\sqrt{\frac{2\lambda}{3}}x} + 1 \right)}{6488\Gamma(4\mu+1) \left(e^{\sqrt{\frac{\lambda}{6}}x} + 1 \right)^8} t^{4\mu} \\
& - \frac{25\hbar^4\lambda^4(\lambda-1)\Gamma(2\mu+1)e^{\sqrt{\frac{2\lambda}{3}}x} \left(11e^{\sqrt{\frac{2\lambda}{3}}x} - 5e^{\sqrt{\frac{\lambda}{6}}x} - 1 \right)}{278\Gamma(\mu+1)^2\Gamma(4\mu+1) \left(e^{\sqrt{\frac{\lambda}{6}}x} + 1 \right)^8} t^{4\mu} \\
& - \frac{125\hbar^4\lambda^4(\lambda-1)\Gamma(3\mu+1)e^{\sqrt{\frac{\lambda}{6}}x} \left(2e^{\sqrt{\frac{\lambda}{6}}x} - 1 \right)}{278\Gamma(\mu+1)\Gamma(2\mu+1)\Gamma(4\mu+1) \left(e^{\sqrt{\frac{\lambda}{6}}x} + 1 \right)^7} t^{4\mu}
\end{aligned}$$

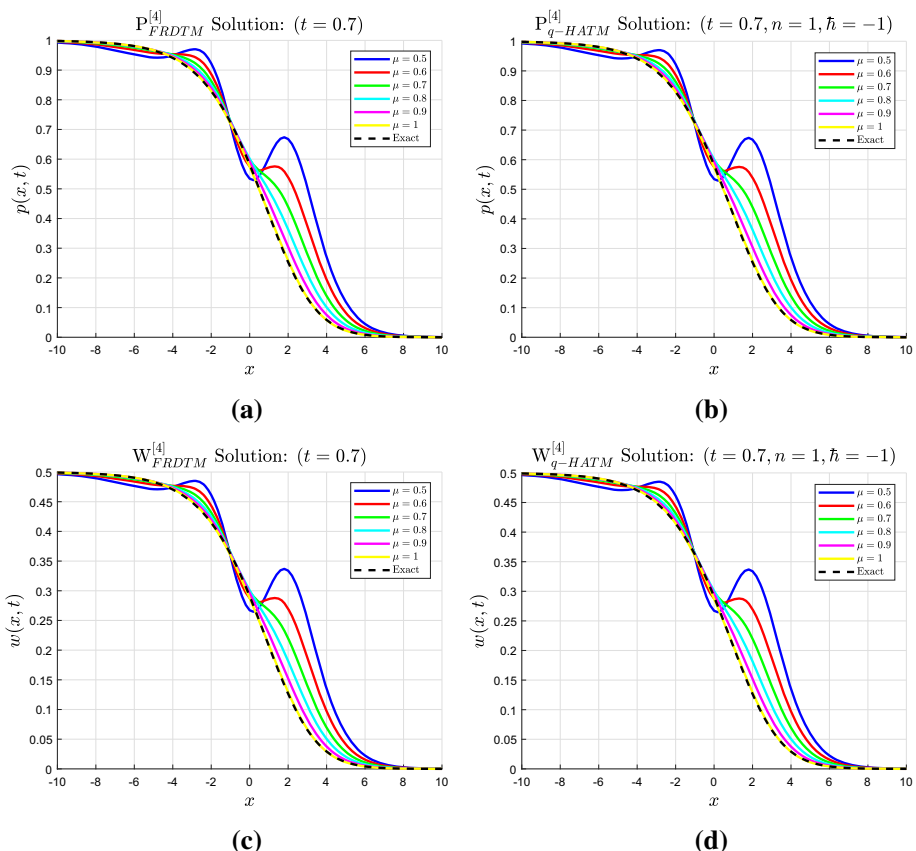


Fig. 10 Solution profiles in **a–d** with different μ values when $t = 0.7$, $\delta = 2$ and $\lambda = 2$ for Case 2

$$+ \frac{25\hbar^4\lambda^4(\lambda-1)e^{\sqrt{\frac{2\lambda}{3}}x}\left(124e^{\sqrt{\frac{2\lambda}{3}}x} + 100e^{2\sqrt{\frac{2\lambda}{3}}x} + 85e^{\sqrt{\frac{\lambda}{6}}x} - 4\right)}{3248\Gamma(4\mu+1)\left(e^{\sqrt{\frac{\lambda}{6}}x} + 1\right)^8}t^{4\mu}.$$

Similar expression for p_m and w_m , respectively, for $m = 5, 6, 7, \dots$ can be achieved. Then for the system of Eq. (38), the \hat{q} -HATM series solution is presented by Eq. (28).

Remark 3 If we let $w = \frac{\lambda-1}{\delta} p$, in Eq. (38), then the system (Case 2) reduces to the fractional Fisher's equation

$$\mathcal{D}_t^\mu p = \frac{\partial^2 p}{\partial x^2} + \lambda p - \lambda p^2, \quad (44)$$

which represents a model for the propagation of a mutant gene where p denotes the population density, $p(1-p)$ stand for the population supply due to births and deaths and λ is the birth rate Fisher (1937). The exact solution of Eq. (44) for the case when $\mu = 1$ can be obtained

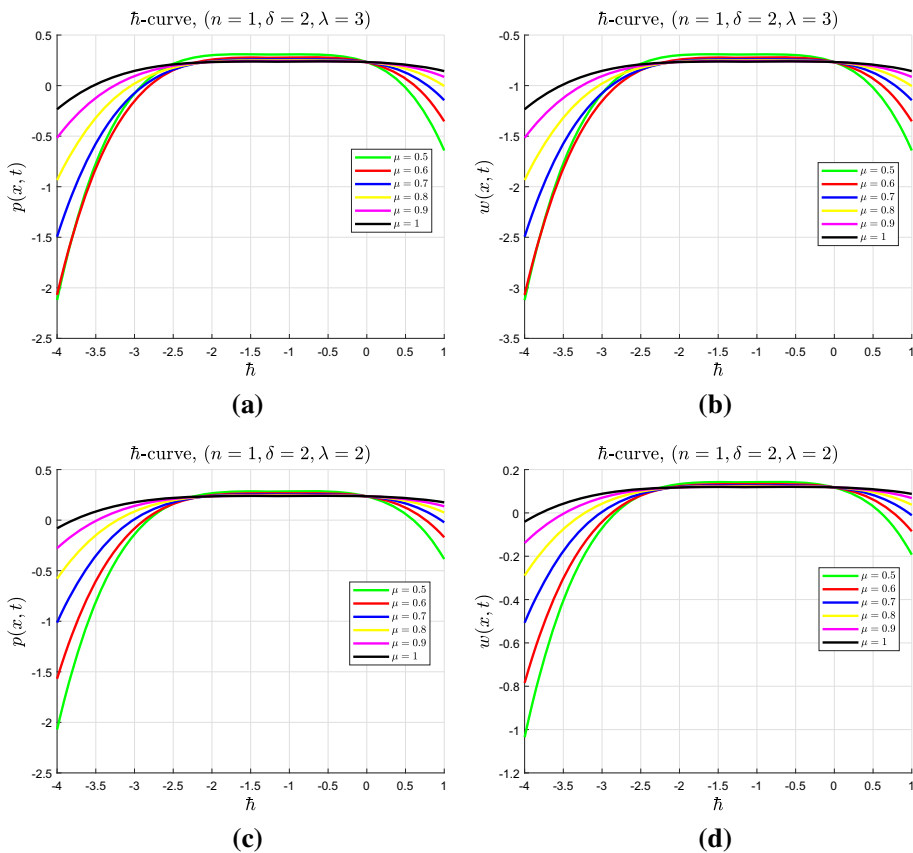


Fig. 11 \hbar -curves plot in **a, b** for Case 1 and in **c, d** for Case 2 when $x = 0.1$, $t = 0.01$ with different μ

from Eq. (40) and is given for positive parameter λ as

$$p(x, t) = \frac{e^{\frac{5\lambda}{3}t}}{\left(e^{\sqrt{\frac{\lambda}{6}}x} + e^{\frac{5\lambda}{6}t}\right)^2} = \frac{1}{4} \left(\tanh \left(\sqrt{\frac{\lambda}{24}}x - \frac{5\lambda}{12}t \right) - 1 \right)^2. \quad (45)$$

5 Numerical results and discussion

Here, the numerical simulation of the obtained results by the two reliable techniques for TFB-Z system of equations is discussed. In Figs. 1, 2, 6 and 7, we observe that for the special case when $\mu = 1$ the difference between the sets of numerical values obtained using the two proposed methods and the exact values are graphically almost indistinguishable. The solution profiles which described the effect and the behavior of the fractional order is presented in Figs. 3, 4, 5, 6, 7, 8, 9 and 10. These solution profiles reveal different behavior for different fractional order μ ($\mu = 0.5, 0.6, 0.7, 0.8, 0.9, 1$), thus assisting in understanding the nature of considered model. From these figures, we notice that as μ increases from 0.5

Table 2 The comparison among FRDTM, q-HATM and the exact solution Eq. (34) for $p(x, t)$ when $\mu = 1$, $n = 1$, $\hbar = -1$, $\lambda = 3$ and $\delta = 2$ for Case 1

| x | t | $P_{\text{FRDTM}}^{[4]}$ | $P_{\text{q-HATM}}^{[4]}$ | p_{Exact} | Absolute error (FRDTM) | Absolute error (q-HATM) |
|-----|------|--------------------------|---------------------------|------------------------------|------------------------------|------------------------------|
| 0.0 | 0.01 | 0.25628873 | 0.25628873 | $2.07040496 \times 10^{-11}$ | $2.07040496 \times 10^{-11}$ | $5.20348487 \times 10^{-09}$ |
| | 0.03 | 0.26909244 | 0.26909245 | $5.20348487 \times 10^{-09}$ | $6.90958160 \times 10^{-08}$ | $6.90958160 \times 10^{-08}$ |
| | 0.05 | 0.28218333 | 0.28218340 | $6.90958160 \times 10^{-08}$ | $2.83274237 \times 10^{-11}$ | $2.83274237 \times 10^{-11}$ |
| | 0.01 | 0.11275577 | 0.11275577 | $6.84093605 \times 10^{-09}$ | $6.84093605 \times 10^{-09}$ | $8.73606064 \times 10^{-08}$ |
| | 0.03 | 0.12043190 | 0.12043189 | $8.73606064 \times 10^{-08}$ | $1.34194669 \times 10^{-11}$ | $1.34194669 \times 10^{-11}$ |
| 1.0 | 0.05 | 0.12848503 | 0.12848495 | $1.33523435 \times 10^{-09}$ | $3.33523435 \times 10^{-09}$ | $3.33523435 \times 10^{-09}$ |
| | 0.01 | 0.03981355 | 0.03981355 | $4.38520725 \times 10^{-08}$ | $4.38520725 \times 10^{-08}$ | $4.38520725 \times 10^{-08}$ |
| | 0.03 | 0.04311413 | 0.04311413 | $2.80693177 \times 10^{-12}$ | $2.80693177 \times 10^{-12}$ | $2.80693177 \times 10^{-12}$ |
| | 0.05 | 0.04664998 | 0.04664993 | $6.64709676 \times 10^{-10}$ | $6.64709676 \times 10^{-10}$ | $6.64709676 \times 10^{-10}$ |
| | 0.01 | 0.01198039 | 0.01198039 | $8.31172891 \times 10^{-09}$ | $8.31172891 \times 10^{-09}$ | $8.31172891 \times 10^{-09}$ |
| 2.0 | 0.03 | 0.01309302 | 0.01309302 | $3.37709548 \times 10^{-12}$ | $3.37709548 \times 10^{-12}$ | $3.37709548 \times 10^{-12}$ |
| | 0.05 | 0.01430171 | 0.01430171 | $8.26454374 \times 10^{-10}$ | $8.26454374 \times 10^{-10}$ | $8.26454374 \times 10^{-10}$ |
| | 0.01 | 0.00326490 | 0.00326490 | $1.07019067 \times 10^{-08}$ | $1.07019067 \times 10^{-08}$ | $1.07019067 \times 10^{-08}$ |
| | 0.03 | 0.00358722 | 0.00358722 | | | |
| | 0.05 | 0.00394024 | 0.00394025 | | | |
| 3.0 | 0.01 | 0.01198039 | 0.01198039 | | | |
| | 0.03 | 0.01309302 | 0.01309302 | | | |
| | 0.05 | 0.01430171 | 0.01430171 | | | |
| | 0.01 | 0.00326490 | 0.00326490 | | | |
| | 0.03 | 0.00358722 | 0.00358722 | | | |
| 4.0 | 0.05 | 0.00394024 | 0.00394025 | | | |

Table 3 The comparison among FRDTM, q-HATM and the exact solution Eq. (34) for $w(x, t)$ when $\mu = 1$, $n = 1$, $h = -1$, $\lambda = 3$ and $\delta = 2$ for Case 1

| x | t | WFRDTM [4] | Wq-HATM [4] | wExact | Absolute error (FRDTM) | Absolute error (q-HATM) |
|-----|------|-------------|-------------|-------------|------------------------------|------------------------------|
| 0.0 | 0.01 | -0.74371127 | -0.74371127 | -0.74371127 | 2.07039941 $\times 10^{-11}$ | 2.07039941 $\times 10^{-11}$ |
| | 0.03 | -0.73090756 | -0.73090755 | -0.73090755 | 5.20348475 $\times 10^{-09}$ | 5.20348475 $\times 10^{-09}$ |
| | 0.05 | -0.71781667 | -0.71781660 | -0.71781660 | 6.90958156 $\times 10^{-08}$ | 6.90958156 $\times 10^{-08}$ |
| | 0.01 | -0.88724423 | -0.88724423 | -0.88724423 | 2.83272295 $\times 10^{-11}$ | 2.83272295 $\times 10^{-11}$ |
| | 0.03 | -0.87956810 | -0.87956811 | -0.87956811 | 6.84093593 $\times 10^{-09}$ | 6.84093593 $\times 10^{-09}$ |
| 1.0 | 0.05 | -0.87151497 | -0.87151505 | -0.87151505 | 8.73606062 $\times 10^{-08}$ | 8.73606062 $\times 10^{-08}$ |
| | 0.01 | -0.96018645 | -0.96018645 | -0.96018645 | 1.34192657 $\times 10^{-11}$ | 1.34192657 $\times 10^{-11}$ |
| | 0.03 | -0.95688587 | -0.95688587 | -0.95688587 | 3.33523398 $\times 10^{-09}$ | 3.33523398 $\times 10^{-09}$ |
| | 0.05 | -0.95335002 | -0.95335002 | -0.95335002 | 4.38520724 $\times 10^{-08}$ | 4.38520724 $\times 10^{-08}$ |
| | 0.01 | -0.98801961 | -0.98801961 | -0.98801961 | 2.80686585 $\times 10^{-12}$ | 2.80686585 $\times 10^{-12}$ |
| 2.0 | 0.03 | -0.98690698 | -0.98690698 | -0.98690698 | 6.64709843 $\times 10^{-10}$ | 6.64709843 $\times 10^{-10}$ |
| | 0.05 | -0.98569829 | -0.98569829 | -0.98569829 | 8.31172919 $\times 10^{-09}$ | 8.31172919 $\times 10^{-09}$ |
| | 0.01 | -0.99673510 | -0.99673510 | -0.99673510 | 3.37729844 $\times 10^{-12}$ | 3.37729844 $\times 10^{-12}$ |
| | 0.03 | -0.99641278 | -0.99641278 | -0.99641278 | 8.26454682 $\times 10^{-10}$ | 8.26454682 $\times 10^{-10}$ |
| | 0.05 | -0.99605976 | -0.99605976 | -0.99605976 | 1.07019068 $\times 10^{-08}$ | 1.07019068 $\times 10^{-08}$ |
| 3.0 | 0.01 | -0.98801961 | -0.98801961 | -0.98801961 | 2.80686585 $\times 10^{-12}$ | 2.80686585 $\times 10^{-12}$ |
| | 0.03 | -0.98690698 | -0.98690698 | -0.98690698 | 6.64709843 $\times 10^{-10}$ | 6.64709843 $\times 10^{-10}$ |
| | 0.05 | -0.98569829 | -0.98569829 | -0.98569829 | 8.31172919 $\times 10^{-09}$ | 8.31172919 $\times 10^{-09}$ |
| | 0.01 | -0.99673510 | -0.99673510 | -0.99673510 | 3.37729844 $\times 10^{-12}$ | 3.37729844 $\times 10^{-12}$ |
| | 0.03 | -0.99641278 | -0.99641278 | -0.99641278 | 8.26454682 $\times 10^{-10}$ | 8.26454682 $\times 10^{-10}$ |
| 4.0 | 0.05 | -0.99605976 | -0.99605976 | -0.99605976 | 1.07019068 $\times 10^{-08}$ | 1.07019068 $\times 10^{-08}$ |

Table 4 The comparison among FRDTM, q-HATM and the exact solution (Eq. (40)) for $p(x, t)$ when $\mu = 1$, $n = 1$, $h = -1$, $\lambda = 2$ and $\delta = 2$ for Case 2

| x | t | $P_{\text{FRDTM}}^{[4]}$ | $P_{\text{q-HATM}}^{[4]}$ | P_{Exact} | Absolute error (FRDTM) | Absolute error (q-HATM) |
|-----|------|--------------------------|---------------------------|--------------------|------------------------------|------------------------------|
| 0.0 | 0.01 | 0.25418393 | 0.25418393 | 0.25418393 | $2.71072054 \times 10^{-12}$ | $2.07040496 \times 10^{-12}$ |
| | 0.03 | 0.26265358 | 0.26265358 | 0.26265358 | $6.73927136 \times 10^{-10}$ | $6.73927136 \times 10^{-10}$ |
| | 0.05 | 0.27125480 | 0.27125480 | 0.27125481 | $8.86035064 \times 10^{-09}$ | $8.86035064 \times 10^{-09}$ |
| | 0.01 | 0.13205178 | 0.13205178 | 0.13205178 | $3.21051519 \times 10^{-12}$ | $3.21051519 \times 10^{-12}$ |
| | 0.03 | 0.13774127 | 0.13774127 | 0.13774127 | $7.72405945 \times 10^{-10}$ | $7.72405945 \times 10^{-10}$ |
| 1.0 | 0.05 | 0.14360140 | 0.14360140 | 0.14360139 | $9.82970280 \times 10^{-09}$ | $9.82970280 \times 10^{-09}$ |
| | 0.01 | 0.05889432 | 0.05889432 | 0.05889432 | $3.00747621 \times 10^{-12}$ | $3.00747621 \times 10^{-12}$ |
| | 0.03 | 0.06193140 | 0.06193140 | 0.06193139 | $7.36736228 \times 10^{-10}$ | $7.36736228 \times 10^{-10}$ |
| | 0.05 | 0.06509804 | 0.06509804 | 0.06509804 | $9.54952466 \times 10^{-09}$ | $9.54952466 \times 10^{-09}$ |
| | 2.0 | 0.02324609 | 0.02324609 | 0.02324609 | $4.48807656 \times 10^{-13}$ | $4.48807656 \times 10^{-13}$ |
| 3.0 | 0.01 | 0.02459380 | 0.02459380 | 0.02459380 | $1.33509275 \times 10^{-10}$ | $1.13509275 \times 10^{-10}$ |
| | 0.03 | 0.02601200 | 0.02601200 | 0.02601200 | $1.51796845 \times 10^{-09}$ | $1.51796845 \times 10^{-09}$ |
| | 0.05 | 0.00841375 | 0.00841375 | 0.00841375 | $5.04100234 \times 10^{-13}$ | $5.04100234 \times 10^{-13}$ |
| | 4.0 | 0.01 | 0.00893812 | 0.00893812 | $1.21954139 \times 10^{-10}$ | $1.21954139 \times 10^{-10}$ |
| | 0.03 | 0.00949336 | 0.00949336 | 0.00949336 | $1.56085945 \times 10^{-09}$ | $1.56085945 \times 10^{-09}$ |

Table 5 The comparison among FRDTM, q-HATM and the exact solution Eq. (40) for $w(x, t)$ when $\mu = 1$, $n = 1$, $h = -1$, $\lambda = 2$ and $\delta = 2$ for Case 2

| x | t | WFRDTM ^[4] | W _q -HATM ^[4] | WExact | Absolute error (FRDTM) | Absolute error (q-HATM) |
|-----|------|-----------------------|-------------------------------------|------------|------------------------------|------------------------------|
| 0.0 | 0.01 | 0.12709197 | 0.12709197 | 0.12709197 | $1.35536027 \times 10^{-12}$ | $1.35536027 \times 10^{-12}$ |
| | 0.03 | 0.13132679 | 0.13132679 | 0.13132679 | $3.36963568 \times 10^{-10}$ | $3.36963568 \times 10^{-10}$ |
| | 0.05 | 0.13562740 | 0.13562740 | 0.13562741 | $4.43016532 \times 10^{-09}$ | $4.43016532 \times 10^{-09}$ |
| | 0.01 | 0.06602589 | 0.06602589 | 0.06602589 | $1.60525759 \times 10^{-12}$ | $1.60525759 \times 10^{-12}$ |
| | 0.03 | 0.06887063 | 0.06887063 | 0.06887063 | $3.86202972 \times 10^{-10}$ | $3.86202972 \times 10^{-10}$ |
| 1.0 | 0.05 | 0.07180070 | 0.07180070 | 0.07180069 | $4.91485140 \times 10^{-09}$ | $4.91485140 \times 10^{-09}$ |
| | 0.01 | 0.02944716 | 0.02944716 | 0.02944716 | $1.50373811 \times 10^{-12}$ | $1.50373811 \times 10^{-12}$ |
| | 0.03 | 0.03096570 | 0.03096570 | 0.03096570 | $3.68368114 \times 10^{-10}$ | $3.68368114 \times 10^{-10}$ |
| | 0.05 | 0.03254902 | 0.03254902 | 0.03254902 | $4.77476233 \times 10^{-09}$ | $4.77476233 \times 10^{-09}$ |
| | 2.0 | 0.01162304 | 0.01162304 | 0.01162304 | $2.24403829 \times 10^{-13}$ | $2.24403829 \times 10^{-13}$ |
| 3.0 | 0.01 | 0.01229690 | 0.01229690 | 0.01229690 | $5.67546374 \times 10^{-11}$ | $5.67546374 \times 10^{-11}$ |
| | 0.03 | 0.01300600 | 0.01300600 | 0.01300600 | $7.58984224 \times 10^{-10}$ | $7.58984224 \times 10^{-10}$ |
| | 0.05 | 0.00420687 | 0.00420687 | 0.00420687 | $2.52050117 \times 10^{-13}$ | $2.52050117 \times 10^{-13}$ |
| | 4.0 | 0.00446906 | 0.00446906 | 0.00446906 | $6.09770697 \times 10^{-11}$ | $6.09770697 \times 10^{-11}$ |
| | 0.05 | 0.00474668 | 0.00474668 | 0.00474668 | $7.80429723 \times 10^{-10}$ | $7.80429723 \times 10^{-10}$ |

Table 6 The error estimate for the time-fractional Fisher's Eq. (44) when $\mu = 1$, $n = 1$, $\hbar = -1$ and $t = 0.001$ for different λ

| x | Absolute error($\lambda = 1$) | | x | Absolute error ($\lambda = 2$) | |
|------|---------------------------------|-------------------------------------|------|----------------------------------|-------------------------------------|
| | PFRDTM ^[4] | P _q -HATM ^[4] | | PFRDTM ^[4] | P _q -HATM ^[4] |
| 0.00 | 5.551115×10^{-17} | 5.551115×10^{-17} | 0.00 | 1.110223×10^{-16} | 1.110223×10^{-16} |
| 0.01 | 2.775558×10^{-17} | 2.775558×10^{-17} | 0.01 | 2.775558×10^{-17} | 2.775558×10^{-17} |
| 0.02 | 5.551115×10^{-17} | 8.326673×10^{-17} | 0.02 | 8.326673×10^{-17} | 8.326673×10^{-17} |
| 0.03 | 5.551115×10^{-17} | 5.551115×10^{-17} | 0.03 | 5.551115×10^{-17} | 5.551115×10^{-17} |
| 0.04 | 5.551115×10^{-17} | 5.551115×10^{-17} | 0.04 | 5.551115×10^{-17} | 5.551115×10^{-17} |
| 0.05 | 2.775558×10^{-17} | 2.775558×10^{-17} | 0.05 | 2.775558×10^{-17} | 2.775558×10^{-17} |

Table 7 The description of numerical solutions obtained from ADM Wazwaz and Gorguis (2004), HPSTM Abedle-Rady et al. (2014), q-HATM (P^[3]) Veerasha et al. (2019), q-HATM (P^[4]), FRDTM and the exact solution at $\mu = 1$, $n = 1$, $\hbar = -1$, $t = 0.001$ and $\lambda = 6$ for the time-fractional Fisher's Eq. (44)

| x | P _{ADM} Wazwaz and Gorguis (2004) | P _{HPSTM} Abedle-Rady et al. (2014) | P _q -HATM ^[3] Veerasha et al. (2019) | P _q -HATM ^[4] | PFRDTM ^[4] | Exact solution |
|------|--|--|--|-------------------------------------|-----------------------|----------------|
| 0.01 | 0.248751565 | 0.248753418 | 0.248751565 | 0.248751565 | 0.248751565 | 0.248751565 |
| 0.02 | 0.246264132 | 0.246265957 | 0.246264132 | 0.246264132 | 0.246264132 | 0.246264132 |
| 0.03 | 0.243789384 | 0.243791181 | 0.243789384 | 0.243789384 | 0.243789384 | 0.243789384 |
| 0.04 | 0.241327440 | 0.241329210 | 0.241327440 | 0.241327440 | 0.241327440 | 0.241327440 |
| 0.05 | 0.238878418 | 0.238880160 | 0.238878418 | 0.238878418 | 0.238878418 | 0.238878418 |

Table 8 The error estimate for the time-fractional Fisher's Eq. (44) when $\mu = 1$, $n = 1$, $\hbar = -1$, $t = 0.001$ and $\lambda = 6$

| x | P _{ADM} Wazwaz and Gorguis (2004) | P _{HPSTM} Abedle-Rady et al. (2014) | P _q -HATM ^[3] Veerasha et al. (2019) | P _q -HATM ^[4] | PFRDTM ^[4] |
|------|--|--|--|-------------------------------------|-------------------------|
| 0.01 | 6.568×10^{-12} | -1.453×10^{-06} | 6.568×10^{-12} | 6.189×10^{-15} | 6.189×10^{-15} |
| 0.02 | 6.629×10^{-12} | -1.825×10^{-06} | 6.629×10^{-12} | 5.912×10^{-15} | 5.912×10^{-15} |
| 0.03 | 6.687×10^{-12} | -1.789×10^{-03} | 6.687×10^{-12} | 5.662×10^{-15} | 5.662×10^{-15} |
| 0.04 | 6.743×10^{-12} | -1.771×10^{-06} | 6.743×10^{-12} | 5.385×10^{-15} | 5.385×10^{-15} |
| 0.05 | 6.796×10^{-12} | -1.743×10^{-06} | 6.796×10^{-12} | 5.190×10^{-15} | 5.190×10^{-15} |

to 1, the solutions obtained by the two methods tends to the integer-order solution which are asymptotically continuously convergent to the exact solution ($\mu = 1$).

To guarantee fast convergence of the series solutions obtained by q-HATM, the choice of the auxiliary parameter \hbar is very vital. The \hbar -curves which guide the optimal choice of the values of \hbar for Cases 1 and 2 are illustrated in Fig. 11. The horizontal line segment in the \hbar -curves presents the range for \hbar (which verifies the choice of selecting $\hbar = -1$ in this present study). In Tables 2, 3, 4 and 5, we present the comparative study among the FRDTM,

q-HATM and the exact solution which indicate the results obtained by the two techniques are very accurate and in agreement with the exact solution for the case when $\mu = 1$. We further present the absolute errors on the cited tables.

Remark 4 In Case 2, the numerical result for the case when $\lambda = 3$ and $\delta = 2$ is identical to the result obtained for $p(x, t)$ in Case 1, so we switch attention to the case when $\lambda = 2$ and $\delta = 2$ instead.

Remark 5 It is worth looking into the numerical solution of the time-fractional Fisher's Eq. (44). Table 6 reveals the absolute error for different λ for the time-fractional Fisher's Eq. (44). In Table 7, the numerical values of the proposed methods is compared to the obtained results by HPSTM Abedle-Rady et al. (2014), q-HATM Veerasha et al. (2019), ADM Wazwaz and Gorguis (2004) and the exact solution. Finally, the comparison in terms of absolute error is presented in Table 8.

6 Concluding remarks

In this paper, the time-fractional Belousov–Zhahotinsky system is solved using two reliable techniques, namely the fractional reduced differential transform method and q-homotopy analysis transform method. Two cases of the model are tested by the proposed methods. The effect of the fractional operator can be observed and capture more interesting physical behaviour of the considered model for diverse arbitrary order. The two methods reveal series form solutions which are stable while the values of the fractional order μ is approaching integer order 1. The outcomes of this study show that the result obtained by q-HATM is more general and contains the result of HAM, ADM, HATM, HPSTM, FRDTM, HPM and RPSM as a special case. The q-HATM uses two parameters \hbar and n that provides flexibility in adjusting and controlling the convergence region of the solution. The choice of these two parameters give q-HATM advantage over these methods.

In Remark 3, it has been shown that the Belousov–Zhahotinsky system for Case 2 can be reduced to the fraction Fisher's equation which represents a model for the propagation of a mutant gene. It is evidence from Tables 7, 8 that the proposed methods outperformed other methods used in obtaining approximate solution of the Fisher's equation. Therefore, the proposed methods used in this present investigation are very effective, accurate and has a wide-ranging feasibility and can solve a lot of strong nonlinear fractional and classical PDEs that arise in physics, chemistry, biology, mathematics, and engineering. As for the future work, the author intend to explore other numerical methods, compare their computational time with the two methods used in this present investigation and study the noise effects with the aim to establish the robustness of the concerned algorithm.

References

- Abedle-Rady AS, Rida SZ, Arafa AAM, Adedl-Rahim HR (2014) Approximate analytical solutions of the fractional nonlinear dispersive equations using homotopy perturbation Sumudu transform method. *Int J Innov Sci Eng Technol* 1(9):257–267
- Adomian G (1994) Solving Frontier problems of physics: the decomposition method. Kluwer, New York
- Akinyemi L (2019) q-Homotopy analysis method for solving the seventh-order time-fractional Lax's Korteweg–de Vries and Sawada–Kotera equations. *Comput Appl Math* 38(4):1–22
- Akinyemi L, Iyiola OS (2020) A reliable technique to study nonlinear time-fractional coupled Korteweg–de Vries equations. *Adv Differ Equ* 169:1–27. <https://doi.org/10.1186/s13662-020-02625-w>

- Akinyemi L, Iyiola OS, Akpan U (2020) Iterative methods for solving fourth- and sixth order time-fractional Cahn–Hilliard equation. *Math Methods Appl Sci* 43(7):4050–4074. <https://doi.org/10.1002/mma.6173>
- Ali M, Alquran M, Jaradat I (2019) Asymptotic-sequentially solution style for the generalized Caputo time-fractional Newell–Whitehead–Segel system. *Adv Differ Equ* 2019:1–9
- Alquran M, Al-Khaled K, Chattopadhyay J (2015) Analytical solutions of fractional population diffusion model: residual power series. *Nonlinear Stud.* 22(1):31–9
- Baleanu D, Guvenc ZB, Machado JT (2010) New trends in nanotechnology and fractional calculus applications. Springer, New York
- Baleanu D, Machado JAT, Luo AC (2011) *Fract Dyn Control*. Springer Science and Business Media, New York
- Baleanu D, Wu GC, Zeng SD (2017) Chaos analysis and asymptotic stability of generalized Caputo fractional differential equations. *Chaos Solitons Fract* 102:99–105
- Caputo M (1969) Elasticita e dissipazione. Zanichelli, Bologna
- Das S (2009) Analytical solution of a fractional diffusion equation by variational iteration method. *Comput Math Appl* 57:483–487
- El-Tawil MA, Huseen SN (2012) The Q-homotopy analysis method (q-HAM). *Int J Appl Math Mech* 8(15):51–75
- El-Tawil MA, Huseen SN (2013) On convergence of the q-homotopy analysis method. *Int J Contemp Math Sci* 8:481–497
- Eltayeb H, Kilicman A (2012) Application of Sumudu decomposition method to solve nonlinear system of partial differential equations. *Abstr Appl Anal* 2012:1–13
- Fisher RA (1937) The wave of advance of advantageous genes. *Ann Eugen* 7(4):355–369
- Gibbs RG (1980) Traveling waves in the Belousov–Zhabotinskii reaction. *SIAM J Appl Math* 38(3):422–444
- He JH (1998) Approximate analytical solution for seepage flow with fractional derivatives in porous media. *Comput Methods Appl Mech Eng* 167:57–68
- He JH (1999) Homotopy perturbation technique. *Comput Methods Appl Mech Eng* 178:257–62
- He JH (2003) Homotopy perturbation method: a new nonlinear analytical technique. *Appl Math Comput* 135:73–9
- Hilfer R, Anton L (1995) Fractional master equations and fractal time random walks. *Phys Rev E* 51:R848–R851
- Iyiola OS (2015) On the solutions of non-linear time-fractional gas dynamic equations: an analytical approach. *Int J Pure Appl Math* 98(4):491–502
- Iyiola OS (2016) Exact and approximate solutions of fractional diffusion equations with fractional reaction terms. *Progr Fract Differ Appl* 2(1):21–30
- Iyiola OS, Soh ME, Enyi CD (2013) Generalised homotopy analysis method (q-HAM) for solving foam drainage equation of time fractional type. *Math Eng Sci Aerosp* 4(4):105
- Jaradat A, Noorani MSM, Alquran M, Jaradat HM (2018a) Numerical investigations for time-fractional nonlinear model arise in physics. *Results Phys* 8:1034–1037
- Jaradat I, Alquran M, Abdel-Muhsen R (2018b) An analytical framework of 2D diffusion, wave-like, telegraph, and Burgers' models with twofold Caputo derivatives ordering. *Nonlinear Dyn* 93(4):1911–1922
- Jaradat I, Alquran M, Al-Khaled K (2018c) An analytical study of physical models with inherited temporal and spatial memory. *Eur Phys J Plus* 133:1–11
- Joseph K (2012) Fractional dynamics: recent advances. World Scientific, Singapore
- Keskin Y, Oturanc G (2010) Reduced differential transform method: a new approach to fractional partial differential equations. *Nonlinear Sci Lett A* 1:61–72
- Khuri SA (2001) A Laplace decomposition algorithm applied to class of nonlinear differential equations. *J Math Appl* 1(4):141–155
- Kilbas AA, Srivastava HM, Trujillo JJ (2006) Theory and applications of fractional differential equations, vol 204. Elsevier Science B.V., Amsterdam
- Kumara D, Singha J, Baleanu D (2017) A new analysis for fractional model of regularized long-wave equation arising in ion acoustic plasma waves. *Math Methods Appl Sci* 40:5642–5653
- Kumar D, Seadawy AR, Joardar AK (2018a) Modified Kudryashov method via new exact solutions for some conformable fractional differential equations arising in mathematical biology. *Chin J Phys* 56(1):75–85
- Kumar D, Singh J, Baleanu D (2018b) A new numerical algorithm for fractional Fitzhugh–Nagumo equation arising in transmission of nerve impulses. *Nonlinear Dyn* 91:307–317
- Kurt A, Rezazadeh H, Şenol M, Neirameh A, Tasbozan O, Eslami M, Mirzazadeh M (2019) Two effective approaches for solving fractional generalized Hirota–Satsuma coupled KdV system arising in interaction of long waves. *J Ocean Eng Sci* 4(1):24–32
- Laskin N, Zaslavsky G (2006) Nonlinear fractional dynamics on a lattice with long range interactions. *Phys A Stat Mech Appl* 368(1):38–54

- Liao SJ (1995) An approximate solution technique not depending on small parameters: a special example. *Int J Nonlinear Mech* 30(3):371–380
- Liao SJ (1998) Homotopy analysis method: a new analytic method for nonlinear problems. *Appl Math Mech* 19:957–962
- Liao SJ (2004) On the homotopy analysis method for nonlinear problems. *Appl Math Comput* 147(2):499–513
- Luchko YF, Srivastava HM (1995) The exact solution of certain differential equations of fractional order by using operational calculus. *Comput Math Appl* 29:73–85
- Mainardi F (2010) Fractional calculus and waves in linear viscoelasticity. Imperial College Press, London
- Miller KS, Ross B (1993) An introduction to fractional calculus and fractional differential equations. Wiley, New York
- Nasrolahpour H (2013) A note on fractional electrodynamics. *Commun Nonlinear Sci Numer Simul* 18:2589–2593
- Podlubny I (1999) Fractional differential equations. Academic Press, New York
- Pu YF (2007) Fractional differential analysis for texture of digital image. *J Algorithm Comput Technol* 1(3):357–380
- Ray SS, Bera RK (2006) Analytical solution of a fractional diffusion equation by Adomian decomposition method. *Appl Math Comput* 174(1):329–336
- Şenol M, İyiola OS, Daei Kasmaei H, Akinyemi L (2019a) Efficient analytical techniques for solving time-fractional nonlinear coupled Jaulent–Miodek system with energy-dependent Schrödinger potential. *Adv Differ Equ* 2019:1–21
- Şenol M, Tasbozan O, Kurt A (2019b) Numerical solutions of fractional Burgers' type equations with conformable derivative. *Chin J Phys* 58:75–84
- Singh J, Kumar D, Baleanu D, Rathore S (2018) An efficient numerical algorithm for the fractional Drinfeld–Sokolov–Wilson equation. *Appl Math Comput* 335:12–24
- Soh ME, Enyi CD, İyiola OS, Audu JD (2014) Approximate analytical solutions of strongly nonlinear fractional BBM–Burger's equations with dissipative term. *Appl Math Sci* 8(155):7715–7726
- Sun HG, Zhang Y, Baleanu D, Chen W, Chen YQ (2018) A new collection of real world applications of fractional calculus in science and engineering. *Commun Nonlinear Sci Numer Simul* 64:213–231
- Sweilam NH, Hasan MMA, Baleanu D (2017) New studies for general fractional financial models of awareness and trial advertising decisions. *Chaos Solitons Fract* 104:772–784
- Tarasov VE (2006) Gravitational field of fractal distribution of particles. *Celest Mech Dyn Astron* 94(1):1–15
- Ullah A, Chen W, Sun HG, Khan MA (2017) An efficient variational method for restoring images with combined additive and multiplicative noise. *Int J Appl Comput Math* 3(3):1999–2019
- Veerasha P, Prakasha DG, Baskonus HM (2019) Novel simulations to the time-fractional Fisher's equation. *Math Sci* 13(1):33–42
- Wazwaz AM, Gorguis A (2004) An analytic study of Fisher's equation by using Adomian decomposition method. *Appl Math Comput* 154:609–620
- Zhabotinsky Anatol M (2007) Scholarpedia 2(9):1435. <https://doi.org/10.4249/scholarpedia>
- Zhang Y, Pu YF, Hu JR, Zhou JL (2012) A class of fractional-order variational image in-painting models. *Appl Math Inf Sci* 6(2):299–306

Publisher's Note Springer Nature remains neutral with regard to jurisdictional claims in published maps and institutional affiliations.